Instituto de Estudios Avanzados en Desarrollo

Evaluating Quinoa Crop Yield in the Face of Agro-climatic Stressors Using the NL-CROP Model

By:

Javier Aliaga Lordemann
Adriana Beatriz Caballero Caballero

Series of Working Papers on Development

No. 17/2024

La Paz, October 2024

Evaluating Quinoa Crop Yield in the Face of Agro-climatic Stressors Using the NL-CROP Model*

Javier Aliaga Lordemann**
Adriana Beatriz Caballero Caballero***

Abstract

Crop models are a key tool for developing adaptation strategies in the agriculture sector. With their evolution over time, they have gradually incorporated new approaches and tools. This document develops a non-linear model for simulating the performance of crops with an innovative approach that includes non-linear functions, thus allowing a more realistic representation of agricultural systems. Focusing on quinoa, we use experimental and field data of zones of the Bolivian Altiplano (high plateau) to evaluate different production outcomes under various climatic and agricultural management scenarios that include multiple agro-climatic stressors. The study reveals that the varieties of quinoa adapted to the local conditions of the study areas have better performance than conventional varieties. This underscores the importance of having material that is genetically adapted for facing the impacts of climate change. Additionally, the results show that the NL-CROP model has a satisfactory ability to both reproduce and predict observed quinoa patterns, considering water and thermal stress impacts. This makes the model a key tool for assessing the impact of climate change and also for anticipating the challenges and opportunities that will arise for quinoa in the future, providing valuable assistance in agricultural planning.

JEL codes: Q01, Q10, Q54, O13

Keywords: quinoa, crop yield, climate stressors, crop model, climate change, agricultural management

* This research is part of the project titled *Creating Indigenous Women's Green Jobs Under Low-Carbon COVID-19 Responses and Recovery in the Bolivian Quinoa Sector*, presently being carried out by Fundación INESAD through the sponsorship of International Development Research Centre (IDRC) of Canada. Possible errors are entirely the responsibility of the authors.
** INESAD Associate Researcher (jaliaga@inesad.edu.bo)
*** INESAD Junior Researcher (acaballero@inesad.edu.bo)

Resumen

Los modelos de cultivo son una herramienta clave para desarrollar estrategias de adaptación en el sector agrícola. Con su evolución en el tiempo, han ido incorporando nuevos enfoques y herramientas. Este documento desarrolla un modelo no lineal para simular el desempeño de los cultivos con un enfoque innovador que incorpora funciones no lineales, lo que permite una representación más realista de los mecanismos agrícolas. Con un enfoque en la quinua, usamos datos experimentales y de campo de las zonas del altiplano boliviano para evaluar los niveles de producción bajo diferentes escenarios agroclimáticos que incluyan múltiples estresores. El estudio revela que las variedades de quinua adaptadas a las condiciones locales de las zonas de estudio muestran un mejor desempeño que las variedades convencionales. Esto subraya la importancia de contar con material genéticamente adaptado para enfrentar los impactos del cambio climático. Adicionalmente, los resultados muestran que el modelo NL-CROP es capaz de reproducir de manera satisfactoria los patrones observados de crecimiento y producción de la quinua, y que el modelo también presenta una buena capacidad predictiva, considerando los efectos del estrés hídrico y el estrés térmico. Esto convierte al modelo en una herramienta clave para evaluar el impacto del cambio climático y, además, anticiparse a los desafíos y oportunidades que puedan presentarse para la quinua en el futuro, brindando así una asistencia valiosa para la planificación agrícola.

Código JEL: Q01, Q10, Q54, O13.

Palabras clave: Quinua, rendimiento de cultivo, estresores climáticos, modelo de cultivo, cambio climático, gestión agrícola.

1. Introduction

Agricultural systems worldwide are facing increasing challenges in crop production due to the effects of climate change, climate variability and inadequate management practices. Phenomena such as water and thermal stress, and a greater incidence of pests and diseases are severely affecting the yields of the main crops at the global scale (Lobell and Gourdji, 2012; Tao *et al.*, 2018).

In this document we present the conceptual development of the non-linear model called NL-CROP (Non-Linear Crop Optimization Model), which adopts an innovative and holistic approach to simulating the processes that determine crop growth and yield. Unlike other, traditional linear models, NL-CROP incorporates non-linear functions that capture the complexity inherent to agricultural systems, allowing a more realistic representation of the underlying mechanisms. One of the principal strengths of NL-CROP is its capacity to simulate the synergic and antagonistic effects of water and thermal stress, and the incidence of pests.

The present work applies NL-CROP to assess quinoa yield in Bolivia under different scenarios of climate stress and agricultural management. Bolivia, a country known for producing quinoa (one of the most important Andean crops), faces considerable challenges in terms of the sustainability of its agricultural systems. Given this, it was considered relevant to perform simulations using NL-CROP, with validations at the experimental and field levels, to thus analyze the model's capacity to reproduce the patterns of growth and production observed.

The results obtained show that NL-CROP is capable of satisfactorily simulating quinoa yield under different conditions of water and thermal stress, climate change and the carbon footprint. This is attributable to the inclusion of non-linear functions that represent, more realistically, the complex physiological mechanisms that determine quinoa's response to the environmental factors and management. Also, the model demonstrates a good predictive capacity, making it a valuable tool for evaluating the impacts of climate change on quinoa production at the local and regional levels. By linking NL-CROP with future climate scenarios, it is possible to anticipate the challenges and opportunities that this Andean crop will face under changing environmental conditions.

Below is a presentation of a literature review done concerning the diverse crop yield models. Further ahead, Section 3 contextualizes climate variability and its effect on agricultural production. Section 4 develops the NL-CROP methodological proposal, which is applied in Section 5, where the results obtained for the zones that are the object of this study are shown. Lastly, the conclusions of the analysis are presented and the document ends with a glossary of the terms used in its preparation.

2. Literature review

In this section we present a literature review of the models employed for simulating agricultural crop yield in the face of different stressors (*i.e.*, climate change, climate variability, water stress, thermal stress, and best agricultural practices). Crop simulation models have been widely used for evaluating the impact of environmental changes and of the management practices of agricultural production.

One of the first models widely used was APSIM (Agricultural Production Systems Simulator), which has evolved to influence the new generation of agricultural system simulators (Holzworth *et al.*, 2014). This model integrates diverse components (crops, pastures, livestock, and water resources) for simulating the growth and yield of crops under different conditions.

Another widely used model is DSSAT (Decision Support System for Agrotechnology Transfer), a modelling system for crop processes that has been fundamental for assessing the effects of climate change in agricultural production (Jones *et al.*, 2003). This model integrates information on crops, soil, climate, and management for simulating crop growth and yield.

On its part, the CropSyst model has also been used to evaluate the effects of climate change and management practices in crop yield (Stöckle *et al.*, 2003). The model centers on the biophysical processes that determine crop growth and development. Beyond the crop simulation models, Boote *et al.* (1983) developed an approach for coupling pest models with crop growth simulators, with the aim of predicting yield reductions caused by biotic factors.

Version 4.5 of the decision-making support system for agrotechnology transfer (DSSAT) provides an integrated tool for simulating crop growth and yield under different environmental and management conditions (Hoogenboom *et al.*, 2010). This tool has been widely used by the scientific community.

In the context of climate change, the Agricultural Model Intercomparison and Improvement Project (AgMIP) established protocols and performed pilot studies for assessing uncertainty and improving the crop models (Rosenzweig *et al.*, 2013). This effort has been crucial for progressing in comprehending the impacts of climate change in agriculture. As to uncertainty in the simulation of yield, Asseng *et al.* (2013) analyzed the case of wheat crops under the effects of climate change, highlighting the need for improving crop models. This was an important step for identifying the limitations of the present models and for guiding the development of new, more robust tools.

Along these lines, Antle *et al.* (2014) developed new parsimonious simulation methods with tools for assessing future food and environmental security. These approaches integrate economic, social and environmental aspects, increasing the scope of the traditional crop models. Ewert *et al.* (2011) took on the changes in scale and the linking methods of models for an integrated evaluation of agro-environmental systems. This was fundamental for understanding how impacts at the local level manifest themselves at broader scales and vice versa. On their part, Rötter *et al.* (2011) expressed the need for a fundamental revision of the crop-climate models, stressing the importance of incorporating a greater understanding of the biophysical processes and of the interactions between the different components of the systems. Holzworth *et al.* (2015) examined the current state and future prospects of the models and of the system software of agricultural production, identifying key areas for the development of new tools and approaches.

Rivington and Koo (2010) analyzed the use of crop models for evaluating the impacts of climate change in agriculture. As a result, they highlighted the need for improving the integration of crop models with other climate and environment models. Fodor *et al.* (2017) also made progress in this direction, as they developed an integrated modelling framework for assessing the effects of water and thermal stress in crop yield, thus allowing a more comprehensive assessment of the impacts of climate factors. Semenov and Stratonovitch (2015) employed the SIRIUS crop model for simulating the effects of climate change on wheat yield, consequently underscoring the importance of considering climate variability in evaluating impacts.

Finally, Shibu *et al.* (2010) applied the APSIM model to evaluate the impact of agricultural management practices in crop yield, which has been essential for developing adaptation and mitigation strategies in the agricultural sector.

Crop simulation models have been key tools for understanding and assessing the impacts of climate change, climate variability, water stress, thermal stress, and management practices in agricultural production. The models have evolved in time, incorporating new approaches and tools, and continue to be essential for informing decision-making and for the development of adaptive strategies in the agriculture sector.

3. Climate change and climate variability

The Bolivian Altiplano has arid and semiarid climate conditions that are extremely hard. It also has a very high altitude, with low levels of precipitation, temperatures ranging from -11 °C to 30 °C, 200 days of frost annually, and very poor and saline soil (Jacobsen, 2011). As a result of climate change, the arid conditions are expected to worsen, with an increase in the risk of drought, frost and lack of water, as well as rise in temperatures (Boulanger *et al.*, 2014).

Some projections show an increase in temperature of at least 3 °C by 2100 and a reduction of precipitation from 10 to 30% by the end of this century (Boulanger *et al.*, 2014). The humidity of the soil is also expected to decrease, and more frequent periods of drought are expected (Valdivia *et al.*, 2013). Also, climate variability in the Altiplano has increased, and with it the level of vulnerability for quinoa production (McDowell and Hess, 2012; Boulanger *et al.*, 2014; Twomlow *et al.*, 2008).

In this context, it is necessary to promote adaptive and anticipatory measures that increase the preparedness of systems for facing the climate crisis instead of reacting once events occur (Morton, 2007). Besides, emphasis must be placed on adaptation strategies with a down-up approach, so as to ensure the equitable designation of resources at the community level, and to improve the adaptation capacity of quinoa producers.

With the aim of better understanding the yield trajectories of quinoa crops – in the face of climate change and variability scenarios – agroclimatic simulations were performed adjusting a climograph[1] that allows performing simulations based on the model known as NL-CROP, which is explained in detail in the following section. In general terms, the aim is to incorporate non-linearities when modelling the phenological cycle of the crop, of the Gompertz type. For calibrating the exercise, there are historical records (of 30-35 years) of the weather stations of Uyuni and neighboring zones. Specifically, there are four study zones: i) Pampa Aullagas and Challapata, ii) Patacamaya, iii) Salinas de Garci Mendoza, and iv) Uyuni, Colchacani and Pulacayo.

The simulations are very sensitive to climate parameters, soil compaction, plantation density, and the hydrophilic characteristics of the soils. Thus, these parameters remain stable within the optimal ranges. The analysis of projections of temperature and precipitation were done by means of a statistical scaling analysis, under the limits of the ECHAM5.0 general circulation model and with the conditions defined by the IPCC (2007) for scenario A2[2].

4. Methodology: NL-CROP model

The NL-CROP model seeks to simulate the development and yield of a crop under conditions of water stress, together with a series of edaphic and climate conditions. The model is governed by a non-linear equation of the Gompertz type, which integrates various equations as the result of a "spline function by parts", which makes it a tool that is useful for approximating complex non-linear functions through the union of more simple linear segments (see Figure 1). The solving of NL-CROP is done by means of a "simulation framework", where iterative methods such as that of Newton-Raphson[3], the fixed point method[4] or methods of confidence region[5] compete, in such a way as to find the model's parameters that best adjust to the available data.

[1] The annexes include the respective climographs for each study zone.
[2] This scenario projects an increase in global temperature from 2° C to 5.4° C by 2100, depending on climate sensitivity. Under this scenario, also expected is an increase in the ocean level and changes in precipitation patterns at the regional level.
[3] Newton-Raphson method: This method is based on the local linearization of the non-linear function and iteration until the solution is found.
[4] Fixed point method: consists of finding the fixed point of a non-linear function by means of an iterative process. It employs the notion of "mapping" of the function.
[5] Region of confidence methods: They define a region of confidence around the present solution and minimize the function within this region.

Figure 1: Spline function by S parts

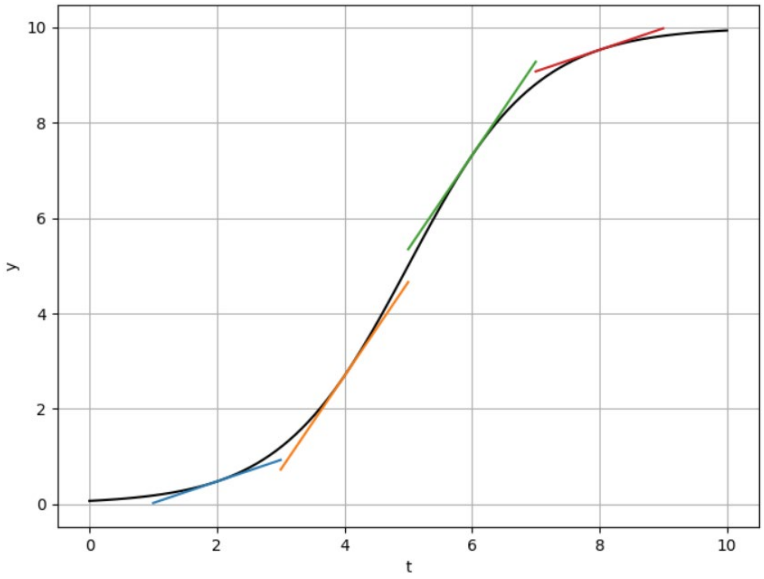

Source: Own elaboration

On its part, this model consists of various equations that simulate crop growth and yield based on data on climate, population density, genetic characteristics, type of soil, level of fertilization, and level of water deficit. Calibrating the model requires monthly or more frequent weather information for a period of over 10 years. This information may be systematized prior to the exercise by preparing a climograph containing maximum temperature (Tmax), minimum temperature (Tmin), precipitation (Pp), and referential evapotranspiration (ETo).

A level of carbon dioxide (CO2) in the atmosphere of 1959 to 2021 is assumed, together with climate change scenarios B1, A1 T, B2, A1 B, A2, and A1 F of the Extreme Events Severity Index (ISEE in Spanish)[6], which are of about 600, 700, 800, 850, 1,250, and 1,550 ppm[7], respectively. If possible, the scenarios may be substituted by specific values, given that the production of biomass and grain depend on the crop parameters, such as stomatal conductance, senescence of the vegetation canopy, water productivity, and the harvest index.

The general equation for estimating crop yield (Y) is Equation (1):

$$Y = Ae^{-be^{-ct}} \quad (1),$$

where:

Y is the potential yield of the crop in the absence of water stress, measured in tons per hectare;
A is the maximum potential or asymptotic yield of the crop;
b determines the point of inflection; that is, the moment at which the crop goes from a slow phase of growth to a more accelerated phase of growth;
c controls the rate growth of the crop; the higher this parameter, the quicker the crop's growth;
t is the time (generally measured in days, weeks or months);
e is the Euler number.

[6] ISEE is an indicator used in the context of climate change for evaluating the severity of extreme climate events such as heat waves, drought, floods, and hurricanes, among others. This index provides a quantitative measure of the magnitude and frequency of such events in relation to a reference period.
[7] parts per million

For example, let us consider a phenological cycle of quinoa of 180 days, with potential yield of 1.2 tons per hectare. Equation (2) would be the one governing the model:

$$Y \cong 1.2\, e^{-be^{-ct}}; (0 \leq t \leq 180) \quad (2)$$

For finding values b and c, we will assume scenarios:

Scenario 1: *b=3* and *c=03*
Scenario 2: *b=4* and *c=05*

These two scenarios allow generating quinoa yield growth curves with different rates of growth and points of inflection, which once linearized approximate the water, edaphic, climate, etc. conditions introduced in the model (see Figure 2).

Figure 2: Quinoa yield growth for both scenarios

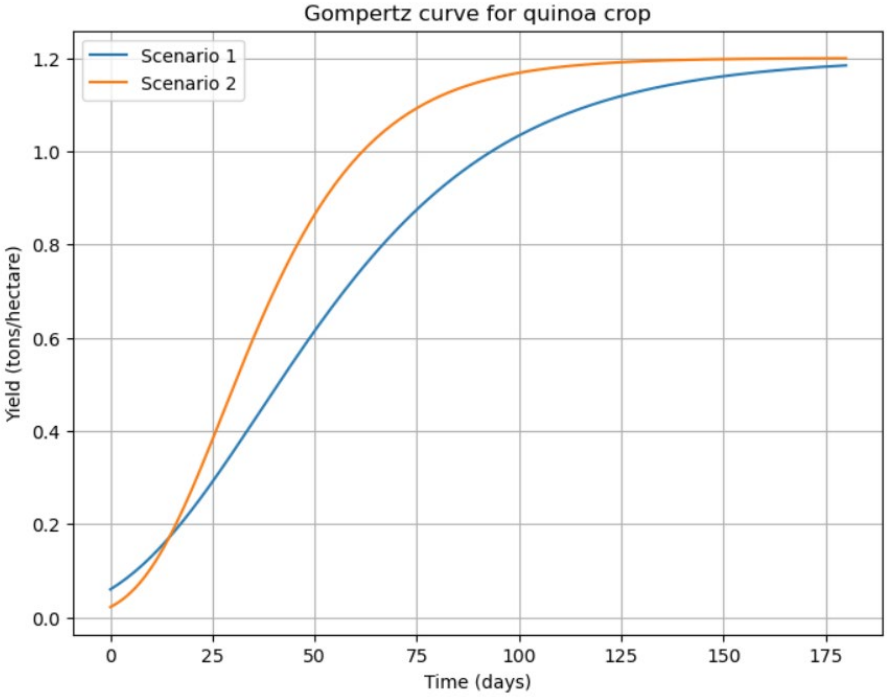

Source: Own elaboration based on the NL-CROP model.

The solution in the NL-CROP model consists of two steps. First, the potential function that governs the crop yield is determined. Second, other equations are included that describe the climate profile, the characteristics of the soil, the management practices, etc. These equations affect parameters *b* and *c* and thus the rate of growth and the inflection in the phenological cycle of the crop; that is, restrictions are imposed on the potential growth. NL-CROP once again simulates with these restrictions, finding an adjusted yield profile that is no longer potential, but rather is constituted by an effective yield.

Effective crop yield

These two resolving steps of the model amount to reformulating Equation (1), which governs quinoa crop yield, in terms of the biomass (*B*) and the harvest index (*H*), as shown in Equation (3):

$$Y = B \cdot H = Ae^{-be^{-ct}} \quad (3),$$

where:

B is the crop's biomass (in tons per hectare);
H is the harvest index, which depends on the specific characteristics of the quinoa crop.

Solving the equation in terms of the biomass gives:

$$B = A_i e^{-be^{-ct}} \quad (4),$$

where now A_i is the effective production of biomass adjusted by the harvest index (in tons per hectare).

Thermal stress

Now, under the new specification, three different answer cases can be considered, depending on what the effect of thermal stress (in terms of an increase in temperature) is in the development of the crop:

i) Inhibition of expansion of the vegetation canopy

This effect can be modelled by means of a factor of reduction of the rate of growth (c), which decreases as thermal stress increases, as shown in Equation (5):

$$B = A_i \, e^{-be^{-c(1-K_1 \cdot T)t}} \quad (5),$$

where K_1 is a parameter that quantifies sensitivity to temperature (T).

ii) Acceleration of senescence of the vegetation canopy

This effect can be modelled by means of a factor of increase of the rate of senescence (b), which increases as thermal stress increases, as shown in Equation (6):

$$B = A_i e^{-b(1+K_2 \cdot T)e^{-ct}} \quad (6),$$

where K_2 is a parameter that quantifies sensitivity to temperature (T).

iii) Stomata closure

This effect can be modelled by means of a factor of reduction in the rate of photosynthesis, which decreases as thermal stress increases, as shown in Equation (7):

$$B = Ae^{-be^{-c(1-K_3 \cdot T)t}} \quad (7),$$

where K_3 is a parameter that quantifies sensitivity to temperature (T).

Water stress

For incorporating the effects of water stress, the model considers a curve that activates when the established limits of soil humidity are reached. It is thus possible to assess the effect of water stress on crop yield throughout its different phases of development, which is useful for planning and evaluating strategies under different conditions of availability of water, irrigation system, type of soil, and date of sowing.

The crop's water requirement is estimated by means of a balance of humidity in the soil which is shown in Equation (8):

$$\theta_{i,j} = \theta_{ij-1} + D + (R + P) + ES + Tr \cdot K \quad (8),$$

where:

$\theta_{i,j}$ is the soil's humidity content at depth level i and moment j ;
D is drainage by deep percolation;
R is irrigation;
P is precipitation;
ES is soil evaporation;
Tr is crop transpiration;
K is an adjustment factor that considers the soil and irrigation system characteristics.

Now we will consider another family of specifications that integrates the water stress effect in the three cases previously mentioned:

i) Inhibition of expansion of the vegetation canopy:

$$B = Ae^{-be^{-c[1-K_1 \cdot T - K_4(\theta_c - \theta)]t}} \quad (9),$$

where:

K_4 is a parameter that quantifies sensitivity to soil humidity deficit $(\theta_c - \theta)$;
θ_c is the critical content of humidity in the soil;
θ is the limit of humidity in the soil (referential value, as it varies by crop).

ii) Acceleration of senescence of the vegetation canopy:

$$B = Ae^{-b[1+K_2 \cdot T + K_5(\theta_c - \theta)] \cdot e^{-ct}} \quad (10),$$

where K_5 is a parameter that quantifies sensitivity to the soil humidity deficit.

iii) Stomata closure:

$$B = Ae^{-be^{-c[1-K_3 \cdot T - K_6(\theta_c - \theta)]t}} \quad (11),$$

where K_6 is a parameter that quantifies sensitivity to the soil humidity deficit.

Growth of the vegetation canopy

On its part, for growth of the vegetation canopy in the NL-CROP model, two cases are assumed: exponential growth, and senescence, that is also exponential. For the modelling Equation, (11) and Equation (12) tend to be used, respectively:

$$CC = CC_0 \, e^{k \cdot LAI} \quad (12),$$

where:

CC is the coverage of vegetation canopy;
CC_0 is the initial coverage of vegetation canopy;
k is the coefficient of light extinction;

LAI is the index of foliar area.

Equation (11) describes the exponential growth of the vegetation canopy as a function of the leaf area index (LAI). As LAI increases, canopy cover (CC) expands exponentially.

The case of exponential senescence of the vegetation canopy (Equation 13):

$$CC = CC_{max}\, e^{-ks \cdot t} \quad (13),$$

where:

CC_{max} is the maximum coverage of the vegetation canopy;
ks is the coefficient of senescence of the vegetation canopy;
t is the time.

Equation (12) describes the senescence or the exponential decrease in the coverage of the vegetation canopy in time. As time progresses, canopy cover decreases exponentially. These equations are based on the works of Monsi and Saeki (1953) and Goudriaan and Van Laar (1994), and are broadly used in crop simulation models for representing the behavior of the vegetation canopy.

Estimation of water needs

The model estimates water needs based on data of the crop coefficient *(kc)* and of potential evapotranspiration *(ETP)*. The first of these is a morphophysiological value particular to each crop, and the second is a variable that depends on the zone's climate (Brouwer *et al.*, 1987; Doorenbos and Pruitt, 1976).

Needed for the crop coefficient is real evapotranspiration (ETR), which in the case of quinoa can be approximated by lysimetry based on the equation of the water balance presented previously (Equation 8), as shown in Equation (14):

$$ETR = (P + R) - D +/- SA \quad (14),$$

where:

ETR is real evapotranspiration;
P is precipitation;
R is irrigation;
D is internal drainage;
SA is variation of water stock in the soil.

Then potential evapotranspiration (*ETP*) is calculated with the following formula (Equation 15):

$$ETP = f(u) \cdot (e_s - e_a) \quad (15),$$

where:

$f(u)$ is a function of wind velocity;
e_s is saturation vapor pressure;
e_a is current vapor pressure.

Thus, the crop coefficient (*kc*) is obtained based on the ratio between real evapotranspiration (*ETR*) and potential evapotranspiration (*ETP*), as shown in Equation (16):

$$k_c = \frac{ETR}{ETP} \quad (16)$$

The integration of the water balance equations in the adjusted non-linear specification in the model will allow estimating with greater precision the water requirements of the quinoa crop. This is achieved based on the relationship between the climate variables (such as potential evapotranspiration) and the morphophysiological characteristics of the plant (reflected in the crop coefficient). Through the incorporation of this section of the calculation of water needs, the adjusted model will be able to more completely simulate crop growth and development. For this, the effects of water and thermal stress must be considered, as well as the dynamics of the vegetation canopy.

Temperature

Finally, calibrating the NL-CROP model requires constructing a climograph, which is a synthesized representation of the climate conditions of a location or region throughout the year. Specifically, a climograph combines and correlates temperature and precipitation information. The climograph allows identifying climate patterns throughout the different seasons of the year; its analysis allows classifying the types of weather (*e.g.*, hot, cold, dry, humid) of a region. Commonly used for maximum and minimum temperatures that affect crops is the Hargreaves-Samani model, summarized by Equation (17):

$$T_{max/min} = T_{mean} \pm 0{,}5 \cdot R_a \sqrt{T_{mean} - T_{min}} \quad (17),$$

where:

$T_{max/min}$ is the maximum or minimum temperature (°C);
T_{mean} is the median daily temperature (°C);
T_{min} is the minimum daily temperature (°C);
R_a is extraterrestrial solar radiation $(MJ/m^2/day)$.

Extraterrestrial solar radiation(R_a) is calculated based on the latitude of the location and the day of the year, employing astronomical equations. This radiation represents the amount of solar energy that reaches the upper part of the atmosphere. Incorporating the Hargreaves-Samani equation into the model allows estimating with greater precision the effect of maximum and minimum temperatures on the quinoa crop growth and development. This, together with the temperature and CO2 equations mentioned previously allows a more complete simulation of the crop's response to climate conditions.

5. Results: agroclimatic scenarios

This section presents the results obtained for each of the study zones: i) Pampa Aullagas and Challapata, ii) Patacamaya, iii) Salinas de Garci Mendoza, and iv) Uyuni, Colchacani and Pulacayo. Applying the NL-CROP methodology specified previously, an analysis is done of the behavior of particular varieties of the quinoa crop in the face of different climate scenarios. For each of the zones, a normal and an alternative quinoa variety are chosen; the latter considered to be more adaptable to climate change. In all cases, the study's assessment is done in the flowering and/or physiological maturity phases, to observe the behavior of the two varieties chosen. The analysis of each of the study zones is made up of three parts: initially, an evaluation is done of the vegetation canopy in the face of variations in soil compaction and fertility; then an analysis is done of the behavior of fresh biomass production and yield under

three scenarios of climate change (Normal, El Niño and La Niña). The exercise is calibrated for a symmetric level of fertility in a range of 65-75%. The three scenarios are derived from the Third Assessment Report of the Intergovernmental Panel on Climate Change (*IPCC*, 2022): a) SIM-1 is the specific estimation of year 0, which corresponds to the current value, 2022; b) SIM-2 is the estimation corresponding to the climate change scenario for the period from 2023 to 2039; c) SIM-3 corresponds to the climate scenario for the period going from 2040 to 2050. Then, crop yield is simulated at different levels, under particular conditions. The study closes with the estimation of CO2 emissions for each yield level.

A. Pampa Aullagas and Challapata

In the Pampa Aullagas and Challapata zone, the Huaycha quinoa variety was chosen for the Normal scenario, and the Pasankalla variety for the alternative scenario. The **Pasankalla** seed is one of the oldest quinoa varieties; its main characteristic is its particular coloring, which goes from blue to brown. This variety develops best in the agroecological zone of Suni in the Altiplano, between 3,815 and 3,900 meters above sea level (masl). On its part, the **Huaycha** seed is small, oval shaped and white-yellowish in color. This seed grows on a plant that can reach two meters in height, with large oval-lanceolate leaves, reddish flowers clustered in loose panicles, and the fruit is in hard capsules resistant to climate change. As to its nutritional profile, the Huaycha seeds are rich in protein, carbohydrates, fiber, amino acids (tryptophan, leucin, arginine, methionine, histidine, and valine), unsaturated fatty acids, vitamins A, C and E, and group B vitamins such as folic acid, thiamine and riboflavin.

In the flowering phase, the maximum canopy is expected to reach a height of between 1.5 and 2.0 m, depending on the variety. Huaycha Grano reaches physiological maturity with a maximum canopy of 73% (see Figure 3); that is, a maximum height of between 1.09 and 1.25 m. On its part, the Pasankalla variety adapts very well to climate change and reaches a maximum canopy of 88%, of 1.65 to 1.70 m.

Figura 3. Canopy coverage by variety type (%)

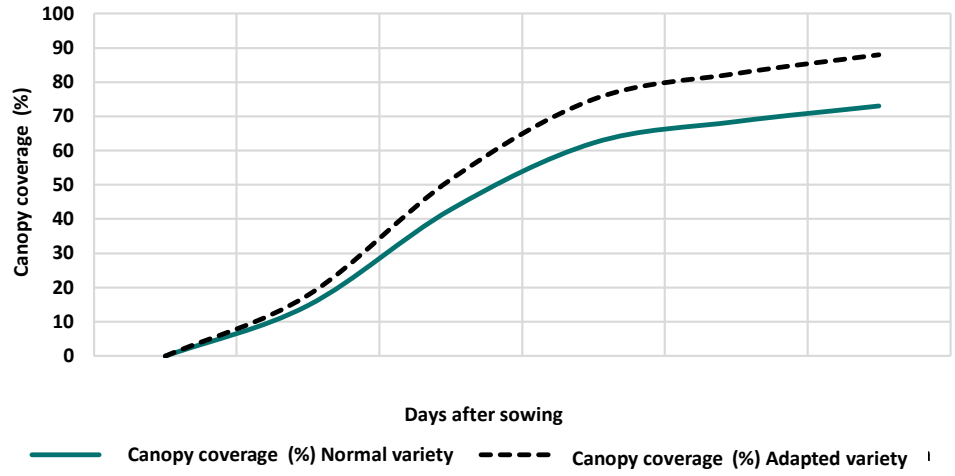

Source: Own elaboration based on the adjusted NL-CROP model.

Figure 4 shows assessment of growth of the canopy cover according to soil porosity and its resistance to the penetration of roots; that is, according to the level of soil compaction[8] – *i.e.*, high, medium and low. For an adequate level of compaction, a canopy of 1.70 to 2.0 m is achieved; that is, with growth to 88%. With the medium compaction level, a

[8] The degree of compaction is determined by the soil dry density and maximum dry density ratio.

canopy of 1.60 to 1.75 m (73%) is reached. The low compaction level (68%) allows a canopy of 1.40 to 1.5 m. In a scenario of cellular atrophy, a canopy reduction of over 40% is expected.

Figure 4. Canopy coverage by compaction level (%)

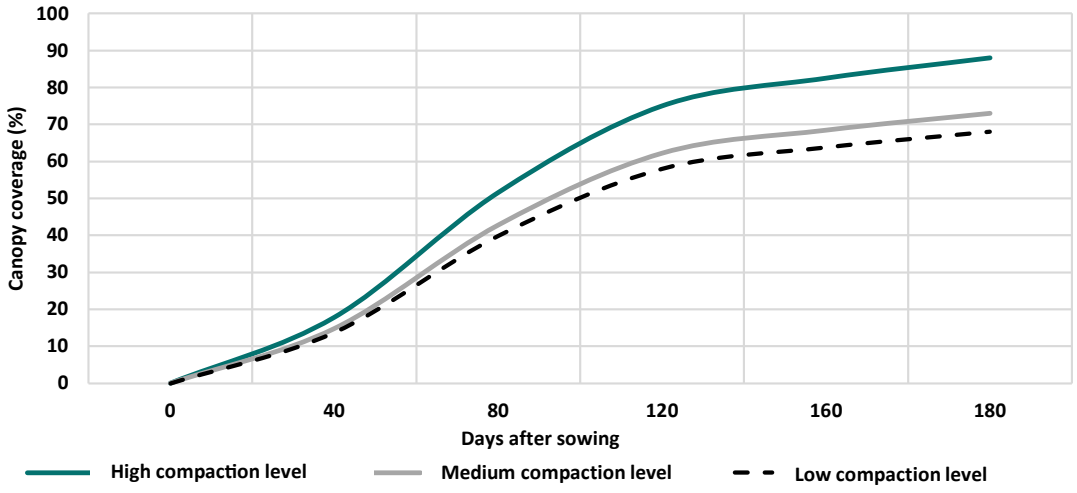

Source: Own elaboration based on the adjusted NL-CROP model.

Figure 5 presents and estimate of canopy cover based on different fertility scenarios. For a fertility level of 83% in the soil, a canopy of 88% is expected (approximately 1.8 m in height). With a soil fertility level of 70%, a canopy with 73% growth is expected (approximately 1.7 m in height). For a low level of fertility (52%), a canopy withy 65-68% growth is expected, with a height of approximately 1.3 m.

Figure 5. Canopy coverage by fertility level (%)

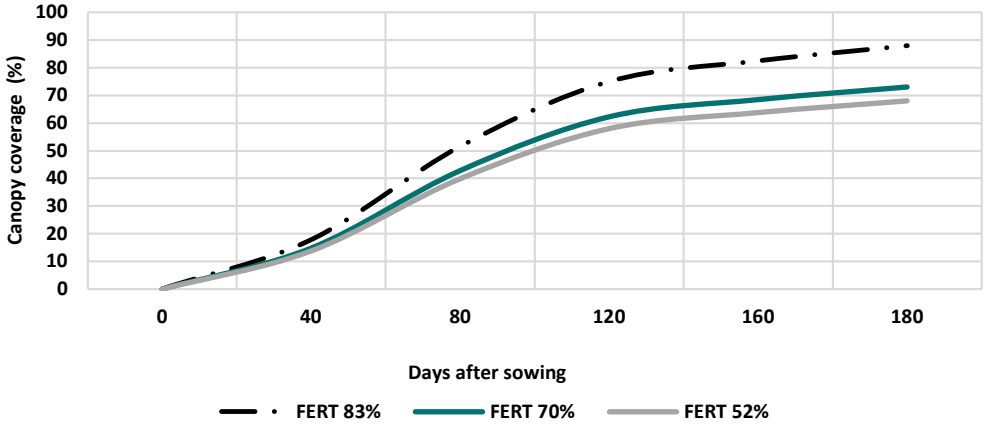

Source: Own elaboration based on the adjusted NL-CROP model.

Figure 6 shows the impact of three climate change scenarios on the production of fresh biomass: Normal or Business as Usual (BAU), La Niña and El Niño, considering the three periods of analysis mentioned: SIM-1 corresponds to the current value of 2022, SIM-2 is the scenario for the 2023-2039 period, and SIM-3 corresponds to the period from 2040 to 2050.

Figure 6. Climate change scenarios (in kg quinoa per hectare)

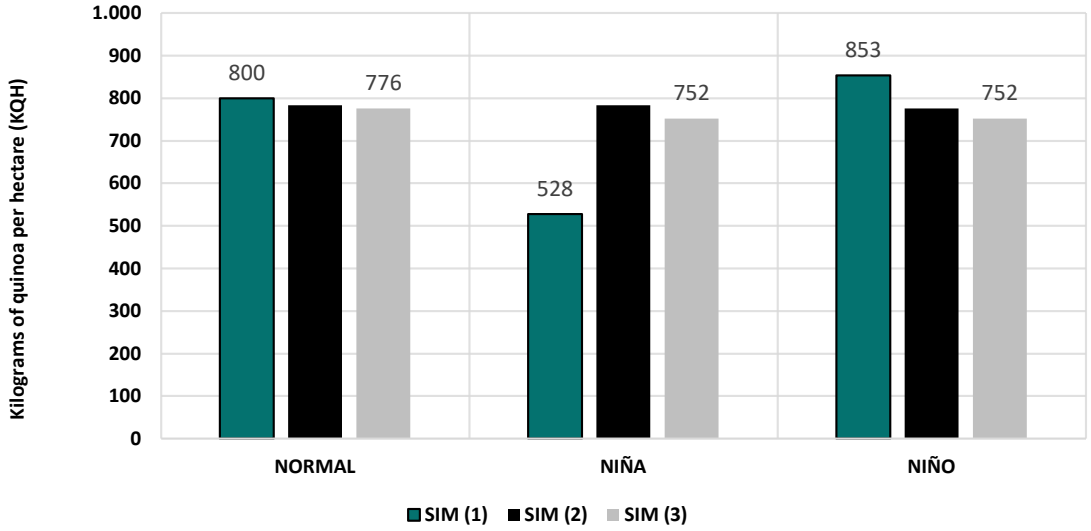

Source: Own elaboration based on the adjusted NL-CROP model.

The results show that climate change reduces crop yield in almost all scenarios. Comparing the Normal scenario in time, we can observe that climate change reduces production from 800 to 776 kilograms of quinoa per hectare (KQH), representing a decrease of 3.01% by 2050.

In the case of the El Niña scenario, an increase of 42% is observed, going from 528 to 752 KQH. Colder than normal temperatures can be expected in the equatorial Pacific Ocean region, which often results in an increase in precipitation in certain areas. Besides, quinoa has use of water efficiency (UWE) of 0.43 kg/m³, which means that it can produce this amount of grains for every cubic meter of water used. Hence, under an El Niña scenario, with more water available, it is likely that quinoa will produce more grains.

For the El Niño scenario, there is a decrease of up to (-)11.8% over the same period; that is, from 853 to 752 KQH. The El Niño phenomenon is characterized by higher than normal temperatures in the equatorial Pacific Ocean region, often leading to a decrease in precipitation in certain areas. In the case of quinoa, an increase in water stress may result in a decrease in yield. The patterns of pests and diseases may also be altered, which can have a negative effect on crop yield.

Figure 7 shows a low yield scenario for levels of fertility of 55% or less, with low levels of organic matter content. Sandy soil is assumed, with a pH range of 6.4 to 7. According to the model, temperature particularly affects the germination phases, given that a minimum of - 4 °C is required. Temperature also affects the flowering phase, causing a low level of pollen production and hence sterility in plants. In the branching phase, decreases in temperature cause no problem at all. The results show that 810 kg of fresh biomass and final yield of 600 KQH are reached.

Figure 7. Low yield (in kg quinoa per hectare)

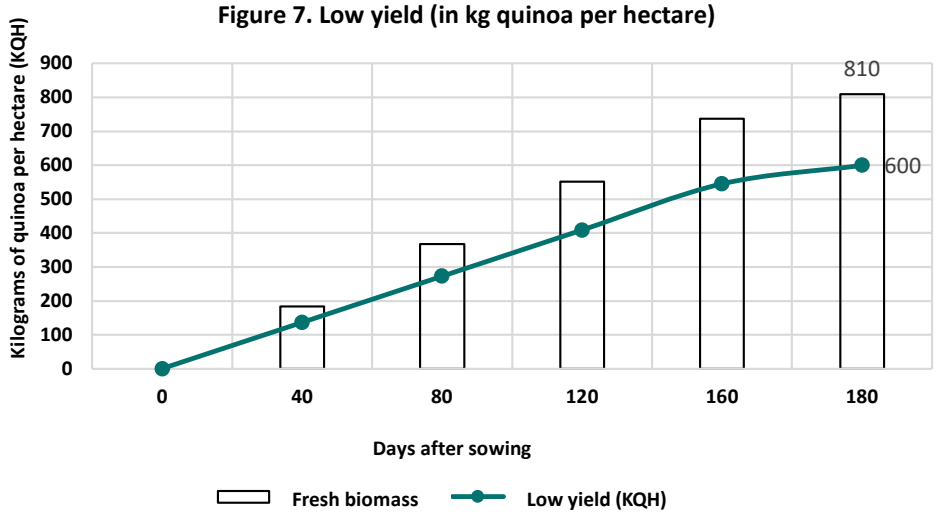

Source: Own elaboration based on the adjusted NL-CROP model.

Figure 8 shows a medium yield scenario for levels of fertility of 60 to 70%, with a moderate content of organic matter. The results show that 1,080 kg of fresh biomass is reached, with a final yield of 800 KQH. In this case, reasonable levels of nitrogen, calcium, phosphorous, and potassium are considered. Besides an average temperature of 25 °C during the day is expected, relative humidity of 87.71% and median annual precipitation of 2,000 mm.

Figura 8. Medium yield (in kg quinoa per hectare)

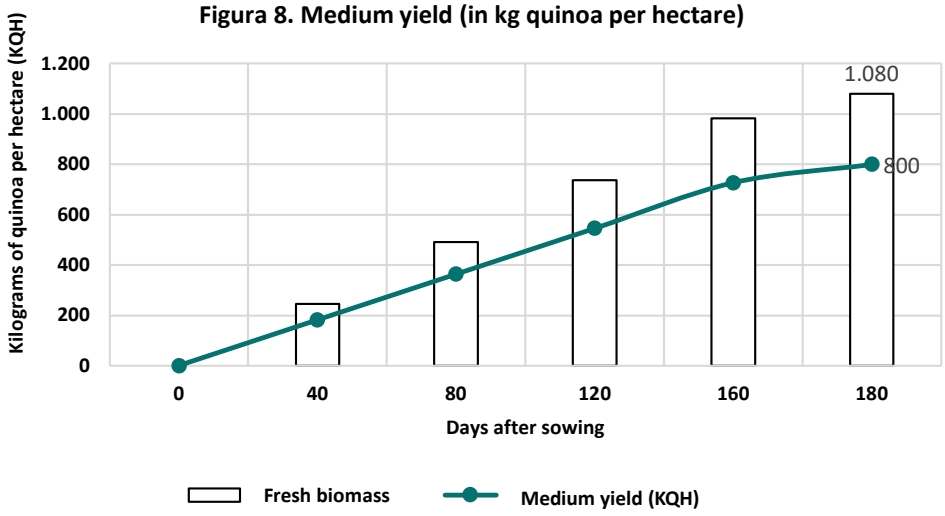

Source: Own elaboration based on the adjusted NL-CROP model.

Figure 9 shows a high yield scenario for levels of fertility of 80% or higher, with adequate organic matter content. The results show that 1,485 kg of fresh biomass is reached, with a final yield of 1,100 KQH with no irrigation in the vegetative cycle. Besides, in this exercise, the potential yield of the crop is calculated under conditions of optimal management, reaching a yield of up to 1,400 KQH.

Figura 9. High yield (in kg quinoa per hectare)

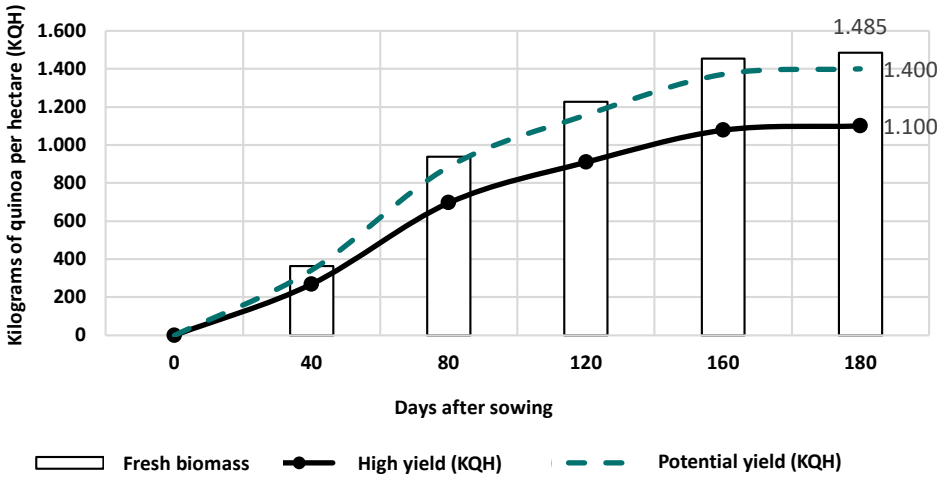

Source: Own elaboration based on the adjusted NL-CROP model.

Finally, Figure 10 estimates CO2eq for three simulated yield scenarios. This is also relevant for evaluating the impact of crops on climate change. One way of measuring this effect is through the greenhouse gas emissions occurring in the production process. For the phenological cycle with low yield, emissions are 1,440 kg of CO2eq per hectare 180 days after sowing. For a medium yield trajectory, reaching 800 KQH in the same time period, emissions are 1,200 kg of CO2eq per hectare. Lastly, for a high yield trajectory, the result is 3,850 kg of CO2eq emissions per hectare.

Figure 10. Emissions per level of coverage (in kg CO2eq)

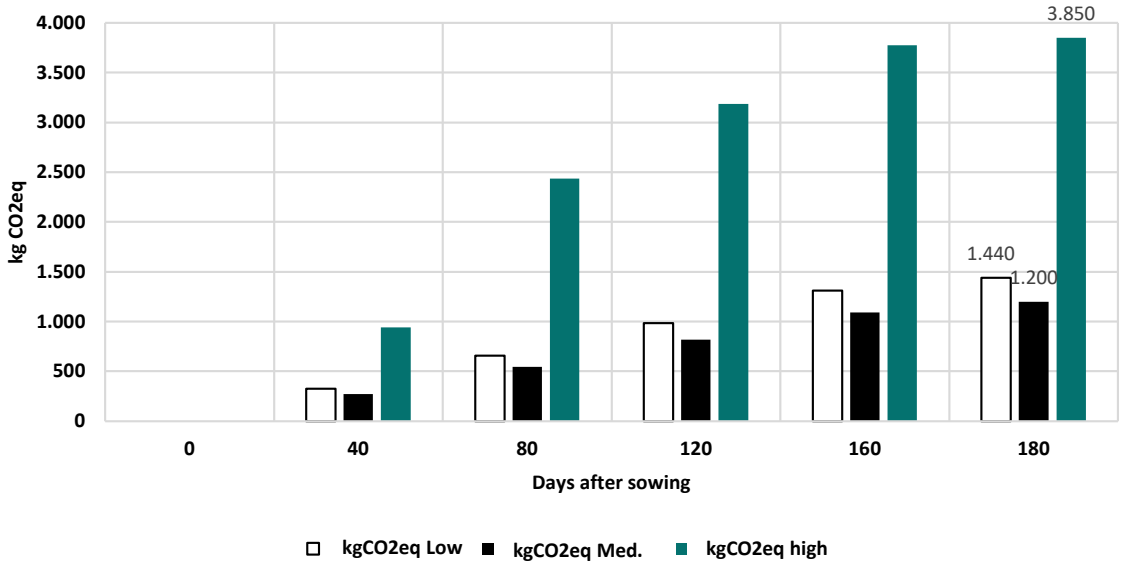

Source: Own elaboration based on the adjusted NL-CROP model.

These estimates show that the optimal scenario considers conditions of a medium yield of 800 KQH six months after sowing, obtaining a lower degree of emissions (1,200 kg of CO2eq per hectare), compared with the situations of low or high yield. Alternatives must be sought to reduce emissions without affecting crop yield; this can be achieved through the implementation of agricultural practices that are environmentally friendly.

B. Patacamaya

For a medium phenological cycle of 180 days, Figure 11 compares the evolution of canopy cover (in percentages) between a normal and a climate adapted quinoa variety. It is worth mentioning that there are many varieties of this grain: Blanquita, Kurmi, Patacamaya, etc.

In the case of the Southern Altiplano, demand for seeds is more variable than in the zones of the Central and Northern Altiplano, because in the south, farmers obtain supplies from their own plots. In other words, although some producers prefer to buy certified seeds, most of them resort to their own seeds for sowing.

In this exercise, **Patacamaya** varieties were chosen for the base exercise, and the **Quinua Real** variety for the alternative scenario. The Patacamaya seed was chosen for its adaptability to the particular climate conditions of the Southern Altiplano[9], including resistance to the cold and its capacity to grow in soil with lower fertility. On its part, Quinua Real is known for its high resistance to adverse climate conditions such as drought and extreme temperatures, which makes it adequate for cultivation in high altitude zones like the Southern Altiplano.

Figure 11. Canopy coverage by variety type (%)

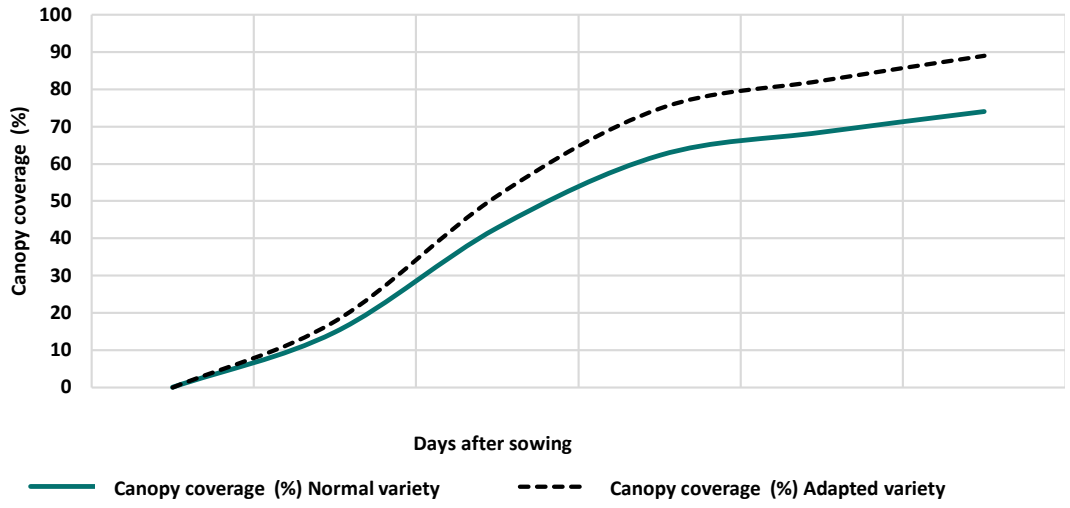

Source: Own elaboration based on the adjusted NL-CROP model.

The maximum canopy is expected to reach a height of between 1.5 and 1.75 m, depending on the variety. Figure 11 shows that the Patacamaya variety reaches physiological maturity with a maximum canopy of 74%, which is a maximum height of 1.45 m. On its part, the Quinua Real variety adapts very well and reaches a maximum canopy of 89%; that is, 1.70 m.

Figure 12 evaluates the growth of canopy cover according to the level of soil compaction – *i.e.*, high, medium and low. With an adequate level of compaction, a canopy of 89% is reached, from 1.53 to 1.64 m. With a medium level of compaction, a canopy of 74% is reached, from 1.14 to 1.37 m; and for a low level of compaction, a canopy of 66% is

[9] In the Southern Altiplano, the local varieties are sown in September, regardless of whether there is rain or snow. In this zone, soil is sandy, and under adequate preparation conditions it stores the humidity resulting from the rains of January and February. The varieties required in the zone are of late or semi-late maturing cycles. When there is faulty emergence or the loss of plots (as a result of burying of seedlings due to wind), re-sowing is done. In such cases, the precocious varieties ("nineties") are the only option, generating a demand for precocious or "nineties" varieties.

reached, which goes from 1.00 to 1.18 m. It is important to mention that the producers are increasingly exposed to episodes of extreme drought which last longer, during which the dry density of the soil increases considerably, resulting in cellular atrophy with canopy growth 38-50% lower, at the medium level.

Figure 12. Canopy coverage by compaction level (%)

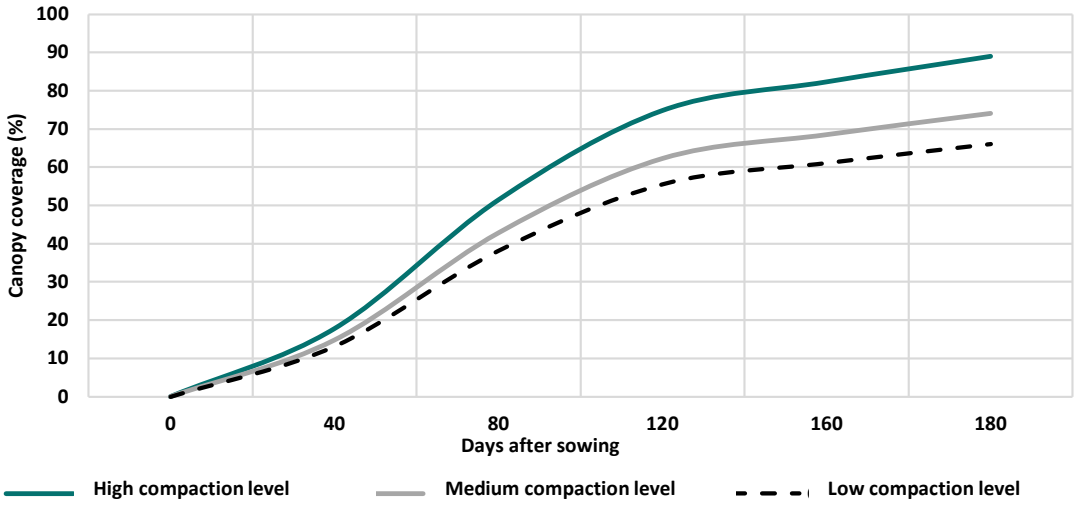

Source: Own elaboration based on the adjusted NL-CROP model.

Figure 13 shows the levels of soil fertility corresponding to the canopy growth trajectories previously defined. For a level of fertility of 84% or more, it is possible to reach a canopy with 89% growth (up to 1.66 m). A soil fertility level of 71% allows reaching a canopy of 74%, with a maximum height of 1.38 m. A low level of fertility of 52-55% permits a canopy with growth of 66%, with a maximum height of 1.10 m.

Figure 13. Canopy coverage by fertility level (%)

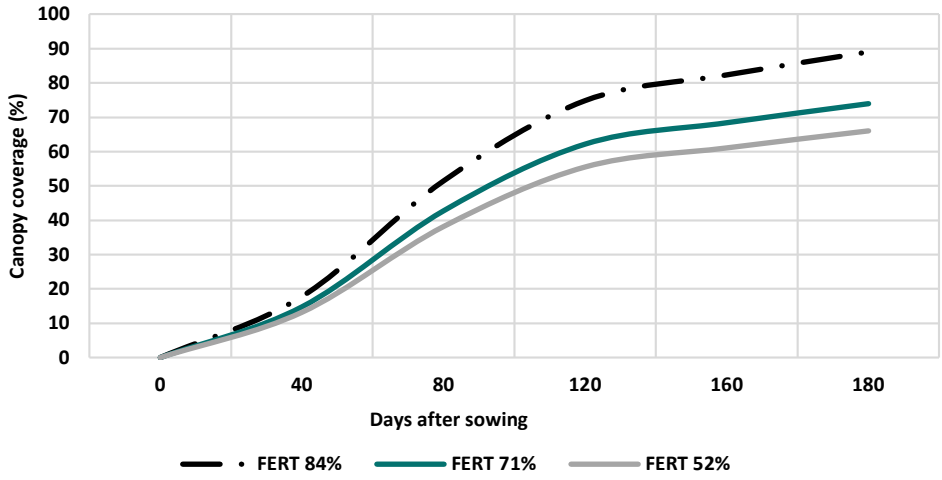

Source: Own elaboration based on the adjusted NL-CROP model.

Figure 14 shows the impact of climate change under the three scenarios considered in the previous case (Normal, La Niña and El Niño) in the production of fresh biomass. The three periods of analysis mentioned are considered: SIM-1 corresponds to the current value of 2022; SIM-2 is the scenario for the 2023-2039 period; and SIM-3 is of the period from 2040 to 2050.

The results show how climate change reduces crop yield under almost all scenarios. Comparing with the Normal scenario in time, it may be observed that climate change reduces production from 600 to 570 KQH, which represents a decrease of (-)5.26% by 2050 (SIM-3). Under the La Niña scenario, an increase of up to 51.6% is observed, while the El Niño scenario presents a decrease of up to (-)22.9% over the same period.

Figure 14. Climate change scenarios (in kg quinoa per hectare)

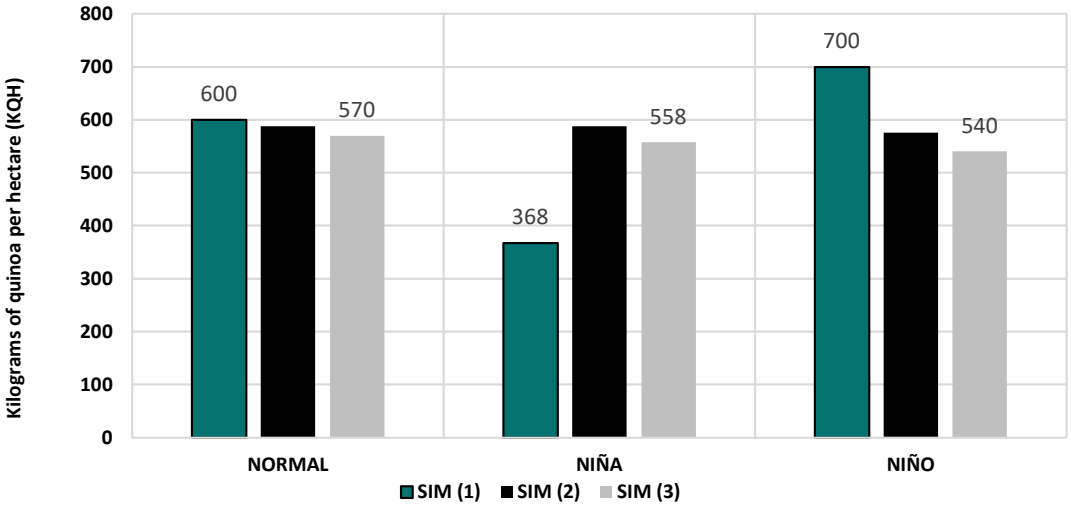

Source: Own elaboration based on the adjusted NL-CROP model.

Figure 15 shows a low yield scenario for levels of fertility of 55% or less, with low organic matter content. The assumption of sandy-clayey soil is made, with a pH level of between 6.5 and 7.5. The climate parameters follow the average trend of the zone's climograph. According to the model, temperature particularly affects the germination phases, as a minimum of - 4 °C is required. The scenario also affects the flowering phase, causing low pollen production, and consequently plant sterility. In the branching phase, drops in temperature do not cause problems. The results show that 472.5 kg of fresh biomass is obtained, with a canopy of 88%, and a yield of 350 KQH.

Figure 15. Low yield (in kg quinoa per hectare)

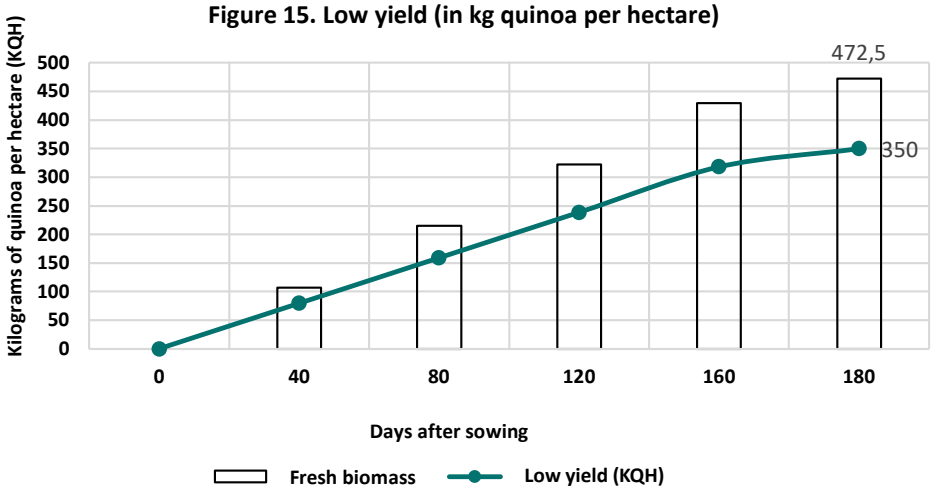

Source: Own elaboration based on the adjusted NL-CROP model.

Figure 16 shows a medium yield scenario for levels of fertility of 60 to 70%, with moderate organic matter content. The soil is assumed to be clay loam with a pH of between 6.5 and 7.5. The climate parameters follow the average trend of the zone's climograph. The results show that 810 kg of fresh biomass is reached, and a final yield of 600 KQH.

Figure 16. Medium yield (in kg quinoa per hectare)

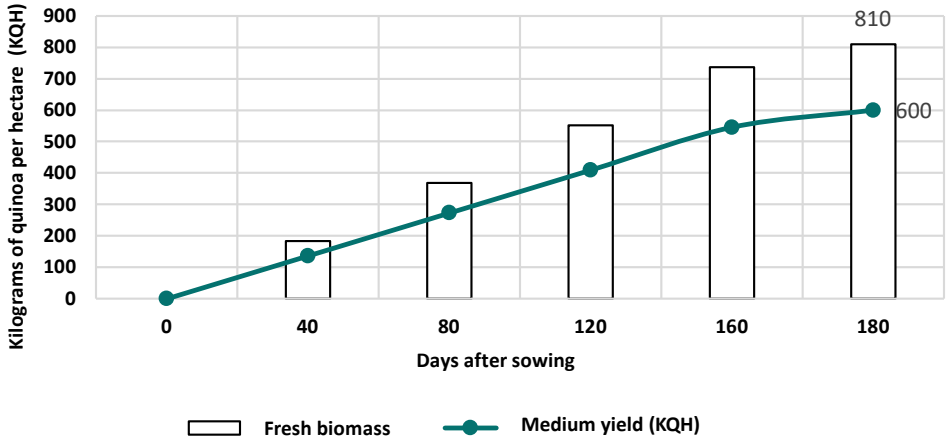

Source: Own elaboration based on the adjusted NL-CROP model.

Figure 17 shows a scenario of high yield for levels of fertility of 80% or more, with adequate content of organic matter. It is assumed that the soil is clay loam, with moderate slopes, and its pH is between 6.5 and 7.5. The climate parameters follow the average trend of the zone's climograph. The results show that 1,021 kg of fresh biomass is achieved, with a final yield of 756 KQH, with no irrigation in the vegetative cycle. Also calculated in this exercise is the potential yield of the crop under irrigation conditions. The application of layers of irrigation show a decrease in the loss of fresh biomass, and a yield of up to 1,150 KQH is obtained.

Figure 17. High yield (in kg quinoa per hectare)

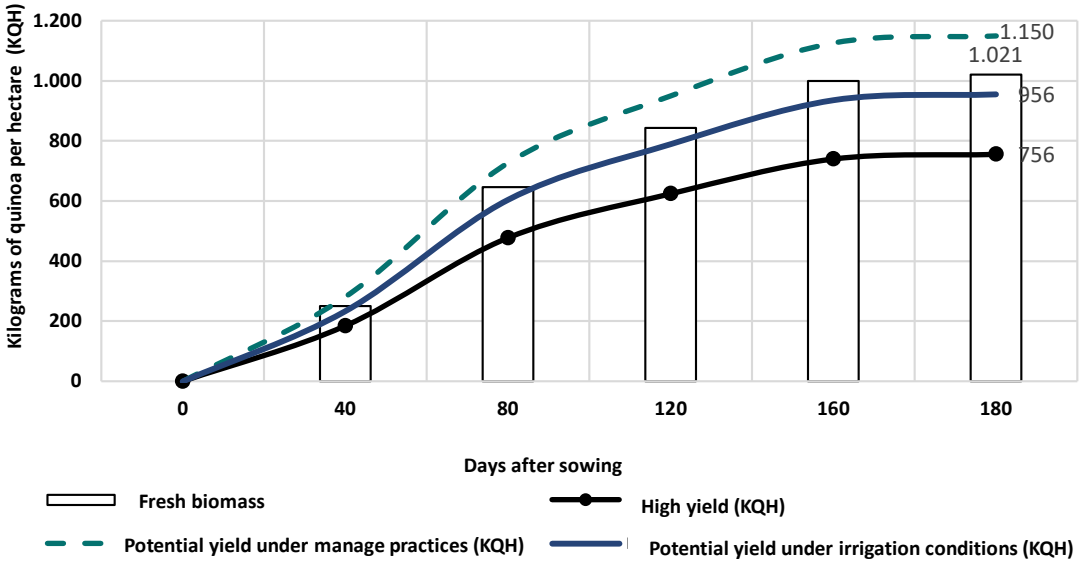

Source: Own elaboration based on the adjusted NL-CROP model.

Figure 18 estimates CO_2eq for the three simulated yields scenarios. For a phenological cycle with low yield, emissions are 525 kg of CO2eq per hectare. With a medium yield trajectory, emissions are 1,446 kg of CO2eq per hectare. Lastly, with a high yield trajectory, 2,700 kg of CO2eq per hectare are obtained. A direct relationship is observed between the crop's level of yield and the corresponding greenhouse gas emission level. The increase in emissions occurs because of the higher intensity of agricultural inputs and practices that are not environmentally friendly. This suggests that the adoption of better agricultural practices increases crop yield without generating an exponential increase in GHG emissions.

Figure 18. Emissions per level of coverage (in kg CO2eq)

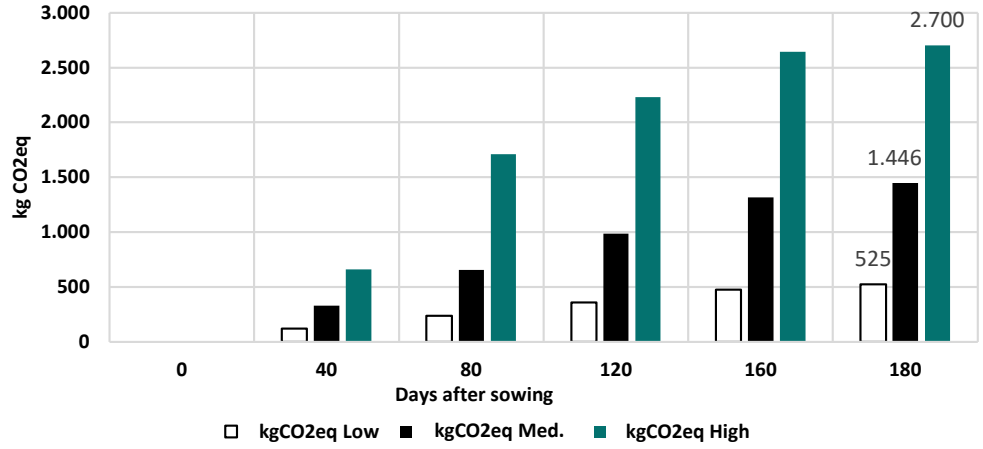

Source: Own elaboration based on the adjusted NL-CROP model.

C. Salinas de Garci Mendoza

Salinas de Garci Mendoza is located between the Uyuni and Coipasa salt lakes, very close to Tunupa and beside the San Pedro and San Pablo mountains. It is a quinoa region by excellence, and has justifiably acquired the name Capital of Royal Quinoa. The Quinua Real variety grows only in this zone and is highly valued in the global markets for being organic and having quality second to none.

For a medium phenological cycle of 180 days, Figure 19 compares the evolution of canopy cover (in percentages) between a normal quinoa variety and one that is climate adapted. At Salinas de Garci Mendoza, quinoa seeds of the following varieties are stored: Kellu, Toledo, Real Blanca, Utusaya, and Pandela. These seeds are strategic for the producer families of the region, known as the Capital of Royal Quinoa.

The Kellu variety adapts well to different climates – including cooler ones – and can withstand lack of irrigation. It also tolerates high levels of salt in the soil, winds and frost, allowing its cultivation in high regions. As with Kellu, the Toledo variety adapts to various climate conditions. On its part, the Utasaya variety adapts to different climates and levels of salinity and can also withstand lack of irrigation.

In this exercise, the **Kellu** and **Toledo** varieties were selected for a normal scenario, and the **Utasaya** variety was used for the alternative scenario. In the flowering phase, the maximum canopy is expected to reach a height of between 1.5 and 1.8 m, depending on the variety. The Kellu and Toledo varieties reach, on average, a maximum canopy of 70%; that is, a maximum height of between 1.0 and 1.3 m. On its part, the Utasaya adapted variety conforms very well, especially to water stress, and reaches a maximum canopy of 89%, between 1.30 and 1.62 m.

Figure 19. Canopy coverage by variety type (%)

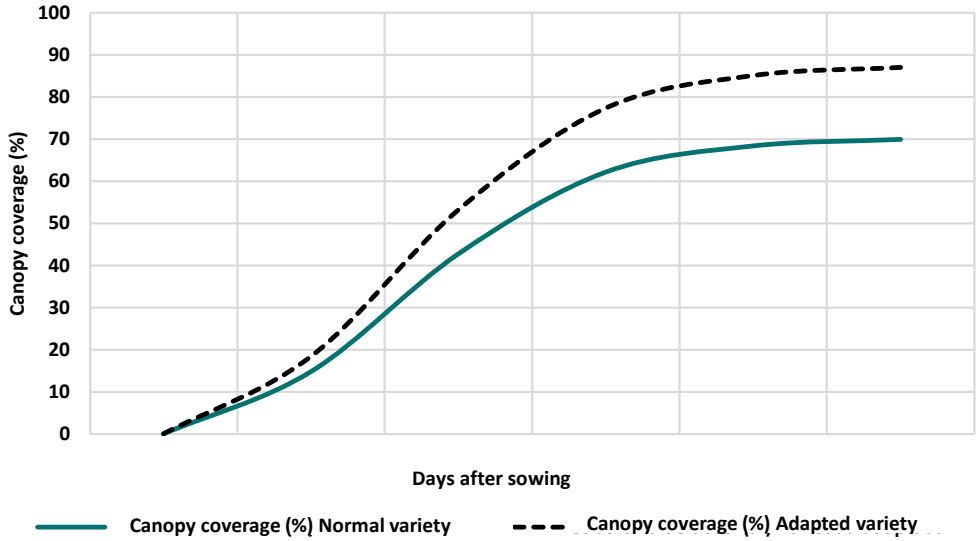

Source: Own elaboration based on the adjusted NL-CROP model.

In Figure 20 we evaluate growth of the canopy cover according to the level of soil compaction – *i.e.*, high, medium and low. For the high level, a canopy of 88.8% is reached, with a height of between 1.30 and 1.60 m. At the medium level of compaction, the canopy level is 70%, with a height of 1.02 to 1.31 m. Finally, with a low compaction level, a canopy of 60.08% is reached, with 0.93 to 1.15 m of height. It is worth mentioning that the producers are increasingly exposed to climate events of greater intensity, particularly prolonged drought, which results in cellular atrophy with canopy growth between 35% and 48% (canopy 54 cm in height or less), with losses in production of up to 88%[10].

Figure 21 evaluates the equivalent levels of soil fertility for the trajectories of canopy growth previously defined. For a level of fertility of 82%, a canopy of 88.2% is reached, with a height of between 1.29 and 1.64 m. For a level of fertility of 69%, a canopy of 70.02% is reached, with height from 1.05 to 1.27 m. Finally, for a low level of soil fertility, of 53-57%, a canopy of 57-62% is reached; that is, a height of approximately 86 cm.

[10] This result was estimated outside the model, as it does not capture canopy growth levels below 60%.

Figure 20. Canopy coverage by compaction level (%)

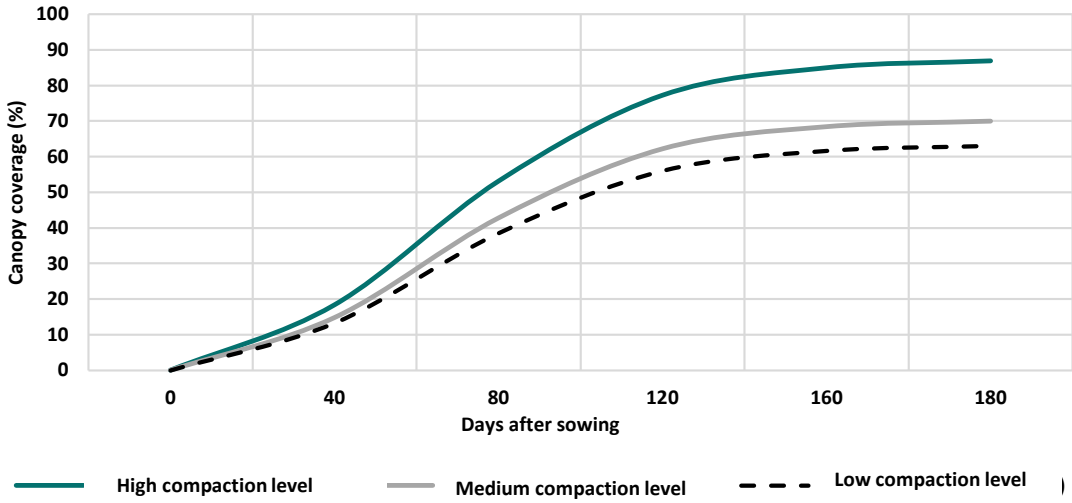

Source: Own elaboration based on the adjusted NL-CROP model.

Soil fertility is closely related to environmental factors and to agricultural practices that have an enormous effect on crops' final yield. In the Salinas de Garci Mendoza zone, the dates for sowing the seeds vary according to climate conditions and the availability of water. Sowing is generally performed in the rainy season, which tends to occur between the months of December and March. During this period, the soil tends to be more humid, favoring the germination of the seeds and growth of the crops.

Figure 21. Canopy coverage by fertiity level (%)

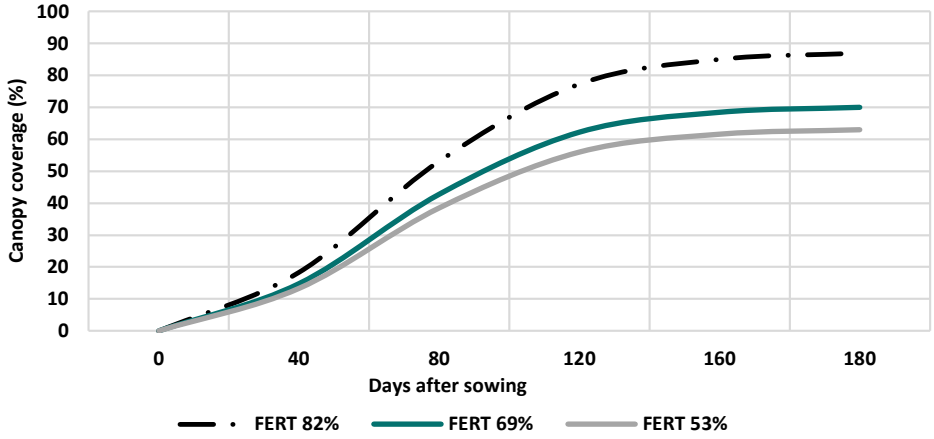

Source: Own elaboration based on the adjusted NL-CROP model.

The soil of the zone is diverse, but is generally characterized by being arid and semiarid, besides having variable levels of fertility. Humidity can be low due to lack of rain in certain periods of the year. In fact, water availability is a crucial factor for crop success in the region, and the farmers tend to depend to a great degree on rain.

The agricultural practices applied in Salinas de Garci Mendoza are unusual, but include techniques such as crop rotation, fallow land, use of organic fertilizers, and sustainable water management. Crop rotation is commonly used for

maintaining the soil's fertility; use of fallow land allows the soil to recover between sowing seasons. The use of organic fertilizers contributes towards improving soil quality, and (once again) sustainable water management is fundamental.

Figure 22 shows the impact of three scenarios of climate change (Normal, La Niña and El Niño) in the production of fresh biomass. The three analysis periods previously mentioned are considered: SIM-1 corresponds to the current value of 2022; SIM-2 is the scenario for the period from 2023 to 2039; and SIM-3 corresponds to the period going from 2040 to 2050. The results show how climate change reduces crop yield under almost all scenarios. In the Normal scenario, compared in time; that is, longitudinally, it may observed that climate change reduces production from 462 to 429.66 KQH, which represents a decrease of 7% by 2050.

In the case of the La Niña scenario, an increase is observed from 262.63 KQH (Normal) to 415.80 KQH, representing an increase of up to 37% only for the superior level of fertility. During a La Niña episode, the zone undergoes an increase in precipitation, leading to greater relative soil humidity. Quinoa is known for its resistance to conditions of humidity and to slightly alkaline soil. La Niña can favor quinoa yield by providing the water needed for the healthy development of crops. Besides, excess humidity in the soil can contribute towards greater plant vigor and an increase in crop productivity.

Figure 22. Climate change scenarios (in kg quinoa por hectare)

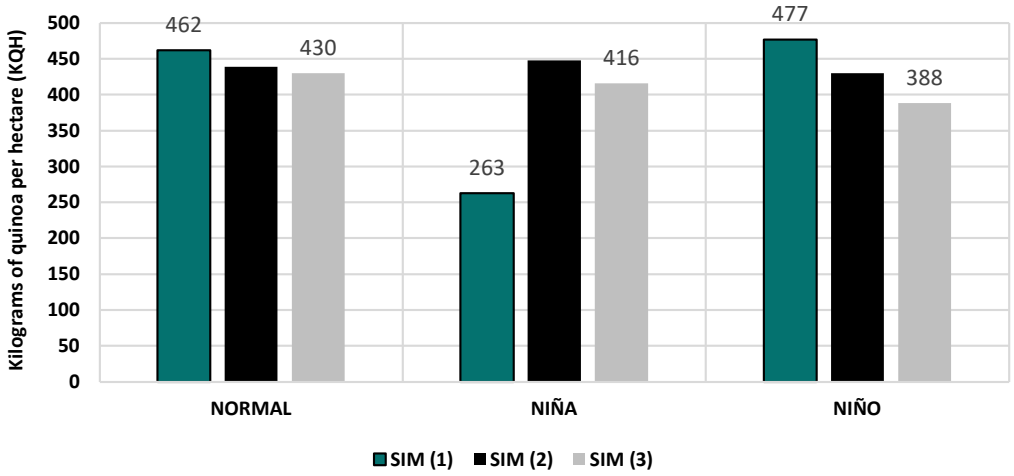

Source: Own elaboration based on the adjusted NL-CROP model.

For the El Niño scenario, there is a decrease of up to (-)18.7% in quinoa yield up to 2050. During El Niño episodes, the zone can undergo prolonged drought and conditions of extreme aridity. Water scarcity can considerably affect the growth and development of crops, resulting in lower yield. Also, the higher temperatures associated with El Niño can cause water stress in quinoa plants, reducing their capacity to absorb nutrients and water, which in turn affects growth and productivity. Finally, it is expected that more days or hours of sunshine accelerate water evaporation in the soil, which contributes to dryer conditions and greater demand for irrigation, possibly leading to lower quinoa yield. These factors, combined with climate change, can have a significant impact on the grain's yield during El Niño episodes, which highlights the importance of implementing adaptation strategies to counter its challenges.

Figure 23 shows a low yield scenario for levels of fertility of 55% or less; that is, those with low levels of organic matter content. The soil of Salinas de Garci Mendoza is characterized by being arid and semiarid. The zone has a slightly alkaline pH, which may affect the availability of nutrients for plants. According to the model, temperature has a particular

effect during the germination phases. It also has an effect during the flowering phase, as it leads to low pollen production, and consequently a greater incidence of plant sterility. The results show that under this scenario, 270 kg of fresh biomass are reached, with a final yield of 200 KQH.

Figure 23. Low yield (in kg quinoa per hectare)

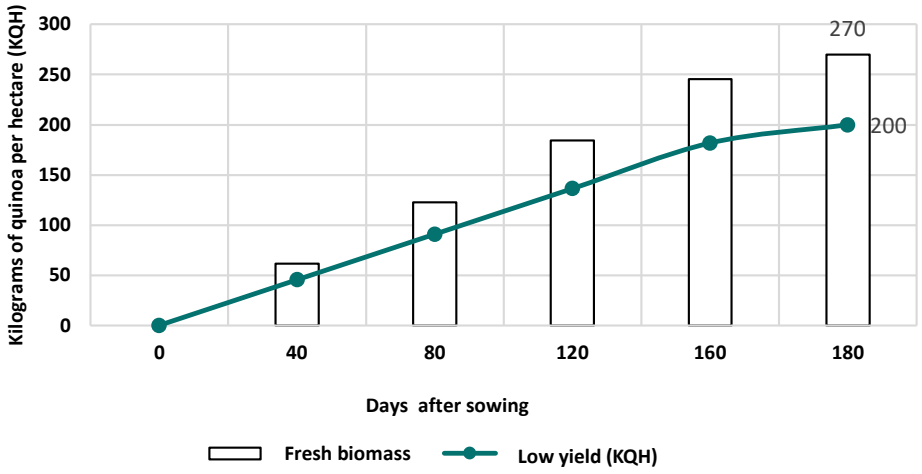

Source: Own elaboration based on the adjusted NL-CROP model.

Figure 24 shows a medium yield scenario for levels of fertility of 60 to 70%, with moderate content of organic matter. The same soil structure and pH levels are assumed. The climate parameters follow the average trend of the zone's climograph. The results show that 623.70 kg of fresh biomass are reached, with canopy not greater than 1.40 m, giving a final yield of 462 KQH.

Figure 24. Medium yield (in kg quinoa per hectare)

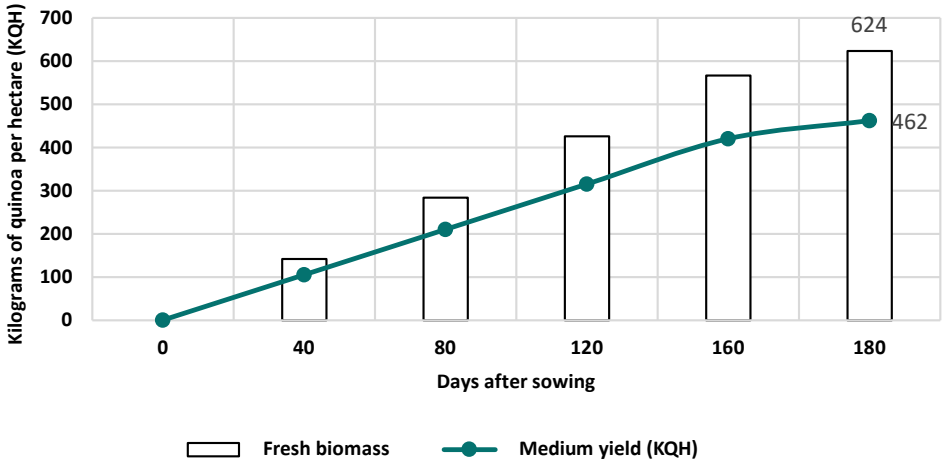

Source: Own elaboration based on the adjusted NL-CROP model.

Figure 25 shows a high yield scenario for levels of fertility of 80% or more, with adequate organic matter content. The same soil structure, pH and climograph are assumed. The results show that 1,109.70 kg of fresh biomass are reached,

with canopy not greater than 1.5 m and a final yield of 822 KQH, with no irrigation in the vegetative cycle. In this exercise, calculation is also done of the crop's potential yield with the implementation of best agricultural practices, which is a yield of 1,150 KQH.

Figure 25. High yield (in kg quinoa per hectare)

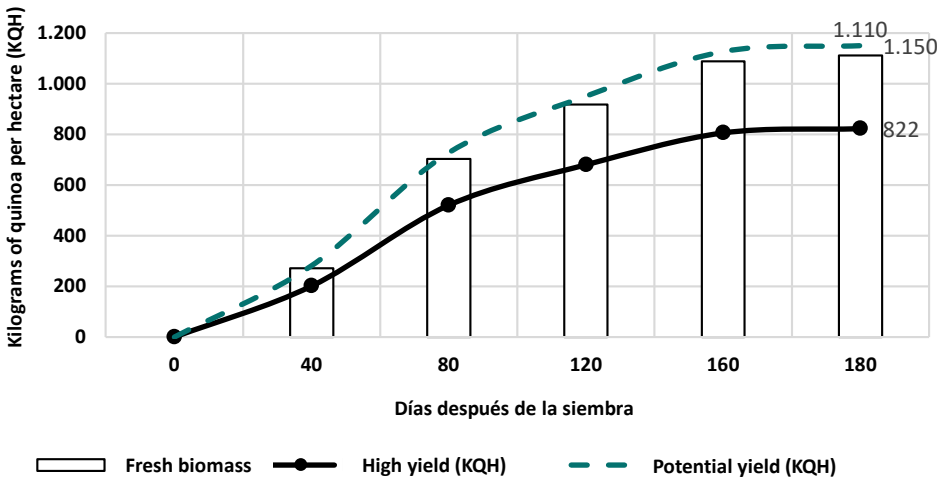

Source: Own elaboration based on the adjusted NL-CROP model.

Figure 26 estimates CO2eq emissions for three simulated yield scenarios. For a phenological cycle with low yield, of 200KQH, emissions are 940 kg of CO2eq per hectare. For a medium yield trajectory equivalent to 462KQH, emissions are 1,386 kg of CO2eq per hectare. Lastly, for a high yield trajectory of 822 KQH, emissions are 4,521 kg of CO2eq per hectare six months after sowing. Once again, an exponential increase is observed in greenhouse gas emissions as the level of crop yield increases.

Figure 26. Emissions per level of coverage (in kg CO2eq)

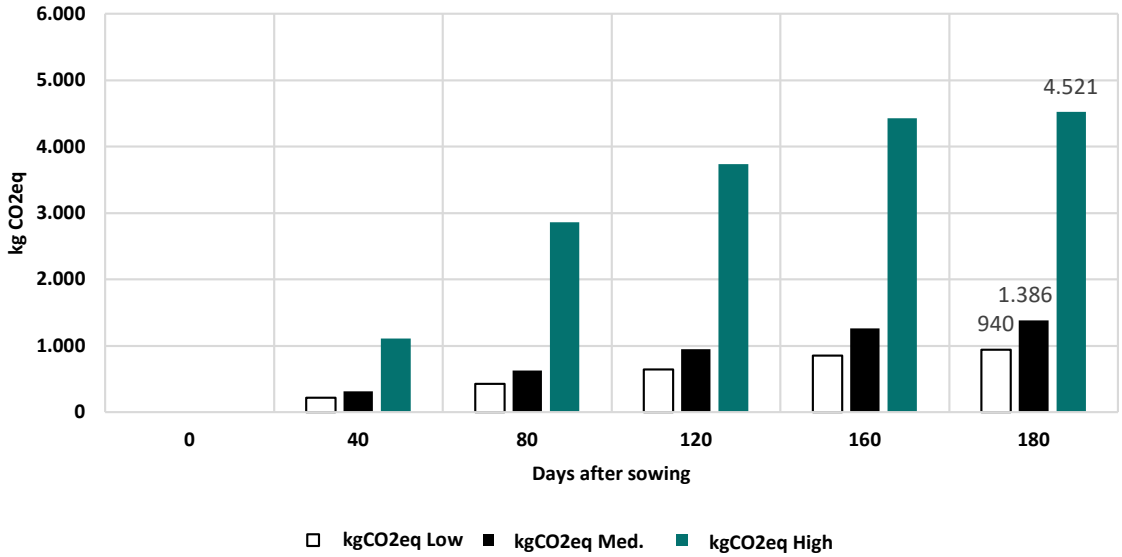

Source: Own elaboration based on the adjusted NL-CROP model.

D. Uyuni, Colchacani and Pulcayo

The region of Uyuni – including the neighboring zones of Colchacani and Pulacayo – are located in the Southern Altiplano of Bolivia, at 3,674 masl. The area corresponds to Köppen and Geiger's Cwb classification, with cold or temperate winters and cool summers. Additionally, summers are rainy and winters dry. At Uyuni and surrounding areas, annual median temperature is 7.76 °C; maximum temperature (Tmax) is 15.24 °C and minimum median temperature (Tmin) is 0.47 °C. Precipitation in normal years fluctuates between 156 and 400 mm/yr.; in dry years it ranges is from 88 to 315 mm/yr.; and in humid years it is between 246 and 493 mm/yr. Based on these parameters, it is estimated that in a normal year Uyuni can have a precipitation deficit of up to 340 mm/yr., with a median level of evapotranspiration of 1.38 mm/day.

For a medium phenological cycle of 180 days, Figure 27 compares the evolution of canopy cover (in percentages) between a normal variety and a climate-adapted[11] one. There are many quinoa varieties; for example, Jach'a Grano, Blanquita, Kurmi, Chucapaca, Aynoca, Patacamaya, Phisancalla, Uyuni, Surumi, Sayaña, Horizontes, Intinaira, and Santa María[12].

Figure 27. Canopy coverage by variety type (%)

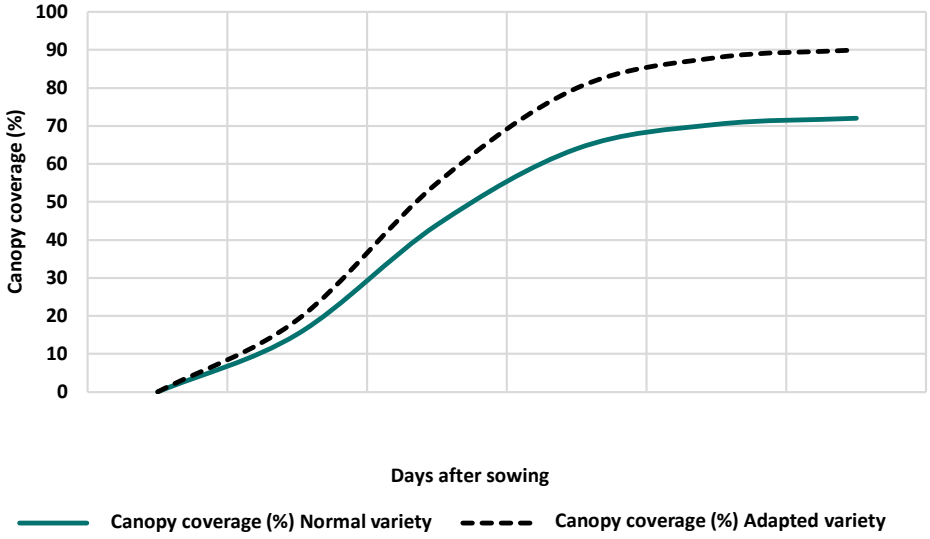

Source: Own elaboration based on the adjusted NL-CROP model.

In this exercise, the **Jach'a Grano** and **Uyuni** varieties were chosen for the normal scenario, which is preferred because it is precocious, has large grains and is partially resistant to mildew. On the other hand, the improved (adapted) varieties are **Horizontes** and **Blanca Real**, thought evidence shows that the Real varieties are susceptible to mildew. Although the seeds and varieties are important in terms of purity, adaptation and viability, environmental factors are

[11] Given the broad genetic diversity of crops, the quinoa varieties differ in the duration of their productive cycles and their resistance to diseases, which determine their differentiated adaptation in production zones.

[12] At the commercial level, sales have been made of the following varieties: Maniqueña, Cariquimeña, Qanchis Blanco, Kurmi, Rosa Blanca, Toledo Rojo, Amarillo Real, Jach'a Grano, Puñete, and Moqu.

also decisive for yield, especially soil fertility and the occurrence of substantial climate events with medium to high severity. These factors are controlled.

In the flowering phase, the maximum canopy height is expected to be between 1.5 and 1.8 m, depending on the variety. The Jach'a Grano variety reaches physiological maturity with a maximum canopy of 72%, with a maximum height of 1.08 to 1.30 m. On its part, the improved varieties adapt very well and reach a maximum canopy of 90%, corresponding to 1.35 to 1.62 m.

In Figure 28 we evaluate the growth of canopy cover according to the level of soil compaction – *i.e.*, high, medium and low. With an adequate level of compaction, canopies reach 1.33 to 1.60 m (90%); 1.06 to 1.31 m (72%) with a medium level, and 0.97 to 1.15 m (65%) with a low level. All values simulated are very robust as compared to the previous exercise. However, producers are increasingly exposed to episodes of severe extreme drought for longer periods of time, which make the dry density of soil increase considerably, leading to cellular atrophy, canopy growth of 38 to 50% – with canopies 57 cm in height or less –, which causes production losses of up to 86%[13].

Figure 28. Canopy coverage by compaction level (%)

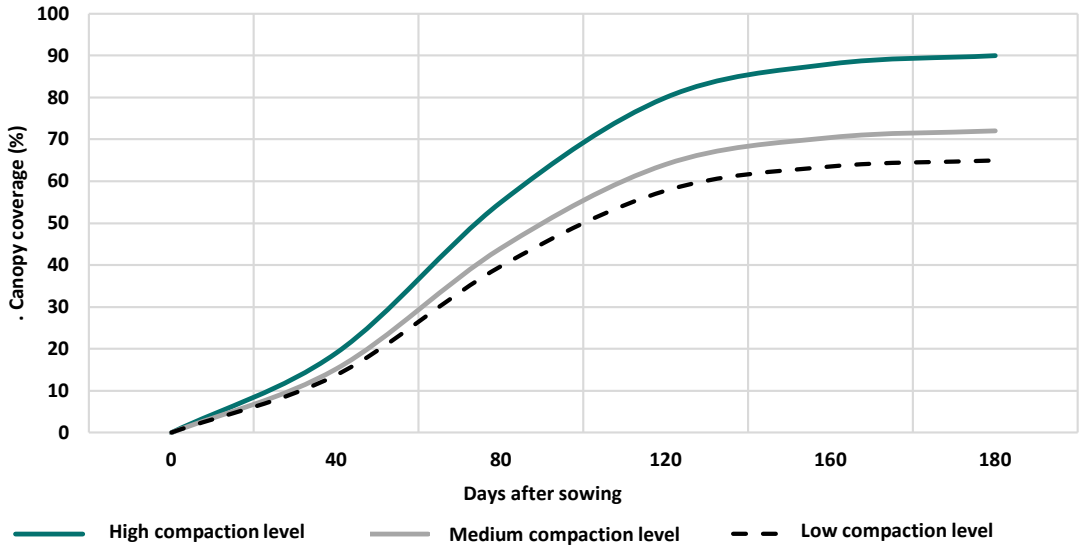

Source: Own elaboration based on the adjusted NL-CROP model.

Figure 29 establishes the levels of equivalent fertility in the soil for the previously defined canopy growth trajectories. For a level of fertility of 85% or more, it is possible to reach canopies of between 1.32 and 1.66 m, equivalent to 90% growth. A level of fertility of 70% allows reaching canopies from 1.08 to 1.30 m (72%), and a low level of fertility of 50-60% allows canopy growth of 60-65%, with an approximate height of 90 cm. In fact, soil fertility is closely related to environmental factors and agricultural practices, which have an enormous effect on the final yield of crops.

[13] This result was estimated outside the model, as it does not capture canopy growth levels below 60%.

Figure 29. Canopy coverage by fertility level (%)

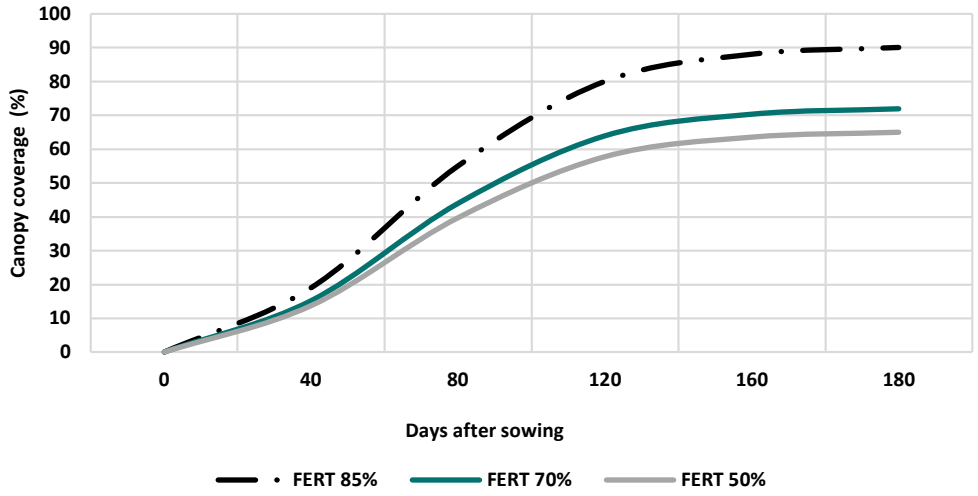

Source: Own elaboration based on the adjusted NL-CROP model.

Figure 30 shows the impact of three climate change scenarios (Normal, La Niña and El Niño) in the production of fresh biomass, considering the three periods of analysis previously mentioned: SIM-1 for the current value of 2022, SIM-2 as the scenario for the 2023-2039 period, and SIM-3 for the period from 2040 to 2050.

Figure 30. Climate change scenarios (in kg quinoa per hectare)

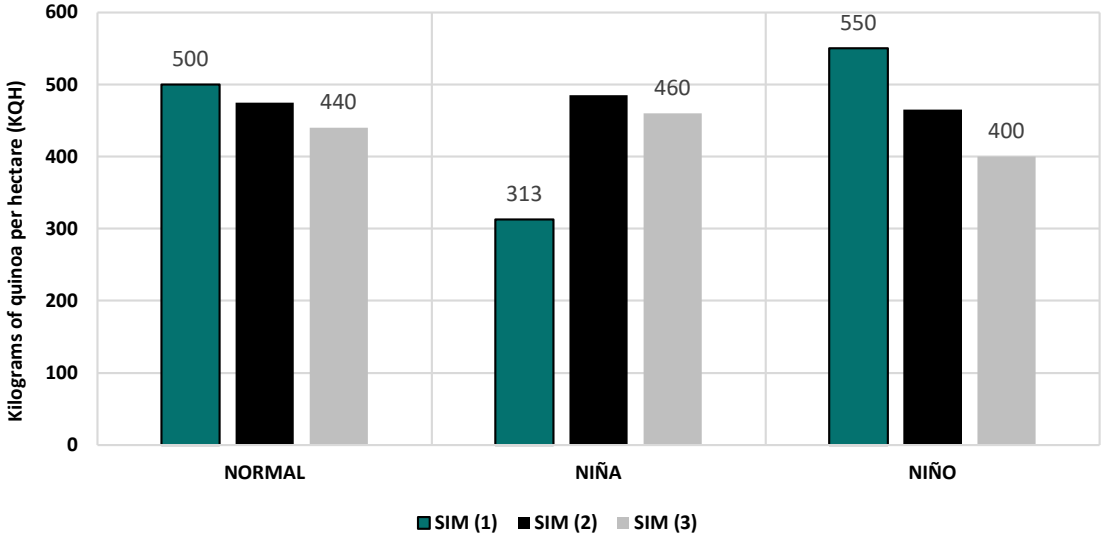

Source: Own elaboration based on the adjusted NL-CROP model.

The results show how climate change reduces crop yield under almost all scenarios. In the Normal scenario, compared in time; that is, longitudinally, it may observed that climate change reduces production from 500 to 440 KQH, which represents a decrease of 12% by 2050.

In the case of the La Niña scenario, an increase of up to 47% is observed due to soil characteristics. A higher level of humidity improves yield, which goes from 313 to 460 KQH.

Under the El Niño scenario, there is a decrease of up to (-)27% in the same period. In such an event, the region can undergo prolonged drought and conditions of extreme aridity. Water scarcity can significantly affect crop growth and development, reducing yield. Also, the higher temperatures associated with El Niño can cause water stress in quinoa plants, reducing their capacity to absorb nutrients and water from the soil, which affects growth and productivity. Finally, it is expected that more days or hours of sunshine accelerate water evaporation in the soil.

Figure 31 shows a scenario of low yield for fertility levels of 55% or less, with moderate to low organic matter (nitrogen). The assumption of clay loam soil is made, with slight slopes and a pH level of between 6.5 and 7.5. The climate parameters follow the average trend of the zone's climograph. According to the model, temperature particularly affects the germination phases, as a minimum of - 4 °C is required. Temperature also affects the flowering phase, causing low pollen production, and consequently plant sterility. In the branching phase, drops in temperature do not cause problems. The results show that 363 kg of fresh biomass are reached, with the canopy not higher than 1.30 m, and a final yield of 269 KQH.

Figure 31. Low yield (in kg quinoa per hectare)

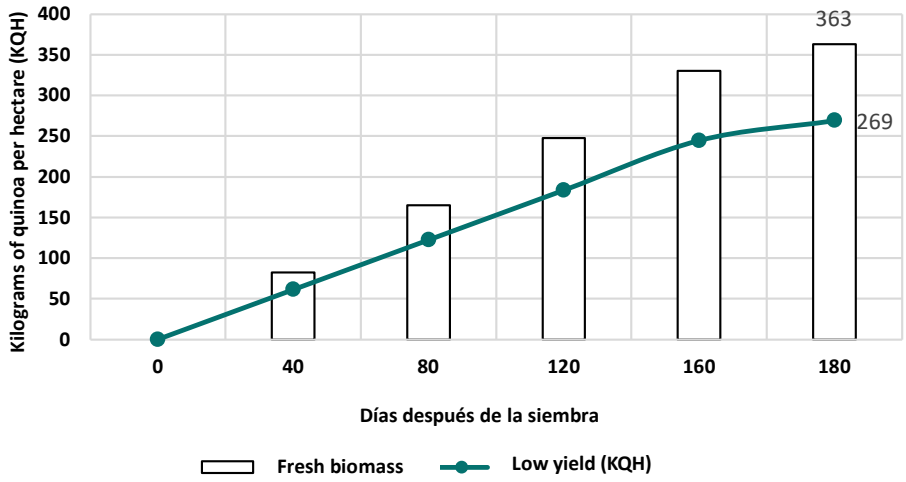

Source: Own elaboration based on the adjusted NL-CROP model.

Figure 32 shows a medium yield scenario for levels of fertility of 60 to 70%, with moderate organic matter content. Clay loam soil is assumed, with moderate slopes and pH of 6.5 to 7.5. The climate parameters follow the average trend of the zone's climograph. The results show that 675 kg of fresh biomass is reached, the canopy is not higher than 1.39 m and final yield is 500 KQH.

Figure 32. Medium yield (in kg quinoa per hectare)

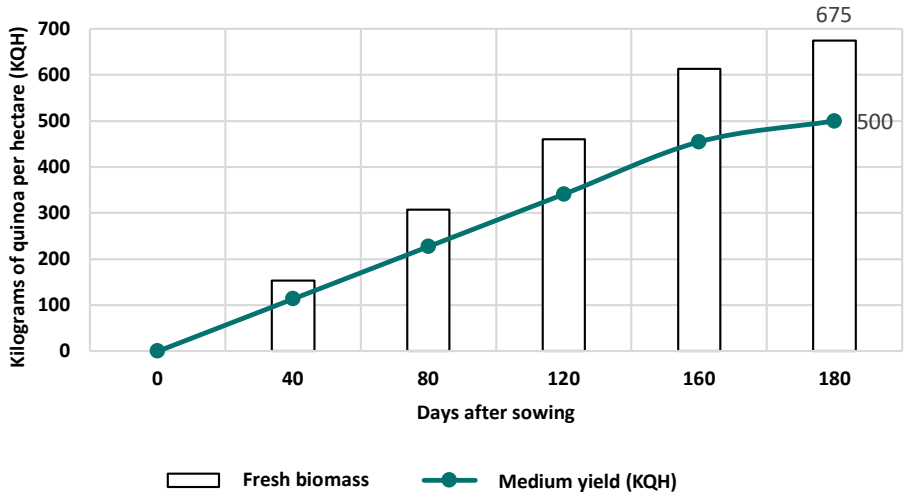

Source: Own elaboration based on the adjusted NL-CROP model.

Figure 33 shows a scenario of high yield for levels of fertility of 80% or more, with adequate content of organic matter. It is assumed that the soil is clay loam, with moderate slopes, and its pH is between 6.5 and 7.5. The climate parameters follow the average trend of the zone's climograph. The results show that 1,021 kg of fresh biomass is achieved, canopy is no higher than 1.48 m, and final yield is 756 KQH, with no irrigation in the vegetative cycle. Also calculated in this exercise is the potential yield of the crop under optimal conditions. The application of layers of irrigation show a decrease in the loss of fresh biomass, with a production of 957 kg, and the application of adequate crop management allows obtaining a yield of up to 1,150 KQH.

Figure 33. High yield (kilograms of quinoa per hectare)

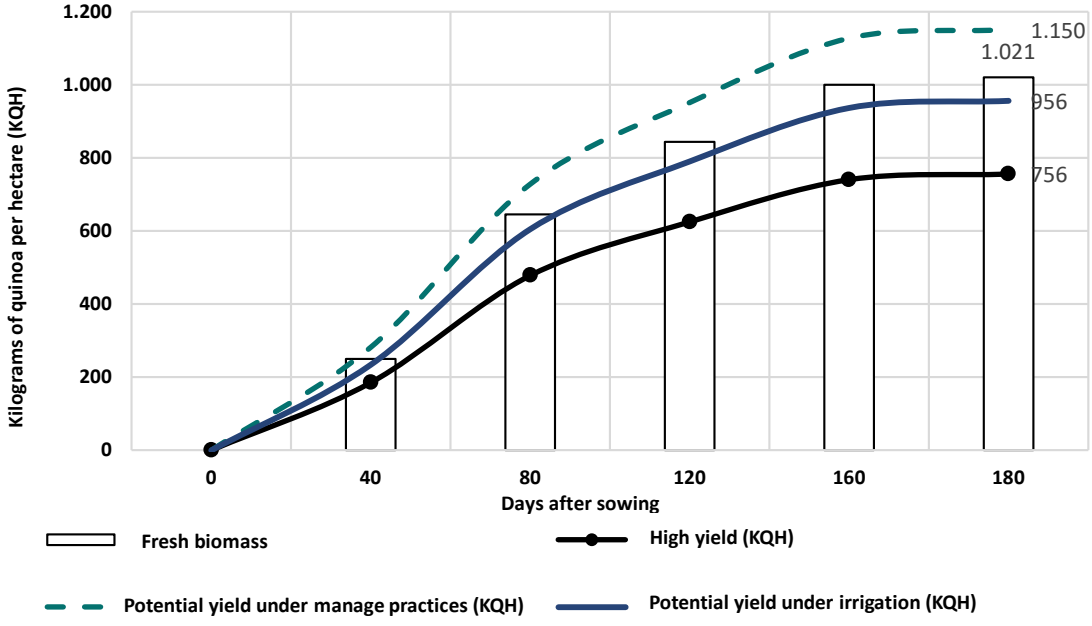

Source: Own elaboration based on the adjusted NL-CROP model.

Finally, Figure 34 estimates CO2eq emissions for the three simulated yield scenarios. For a low yield phenological cycle (269 KQH), emissions are 1,076 kg of CO2eq per hectare. For a medium yield trajectory (500 KQH), emissions are 1,650 kg of CO2eq per hectare. Lastly, for a high yield trajectory (756 KQH), emissions are 4,536 kg of CO2eq per hectare.

Figure 34. Emissions per level of coverage (in kg CO2eq)

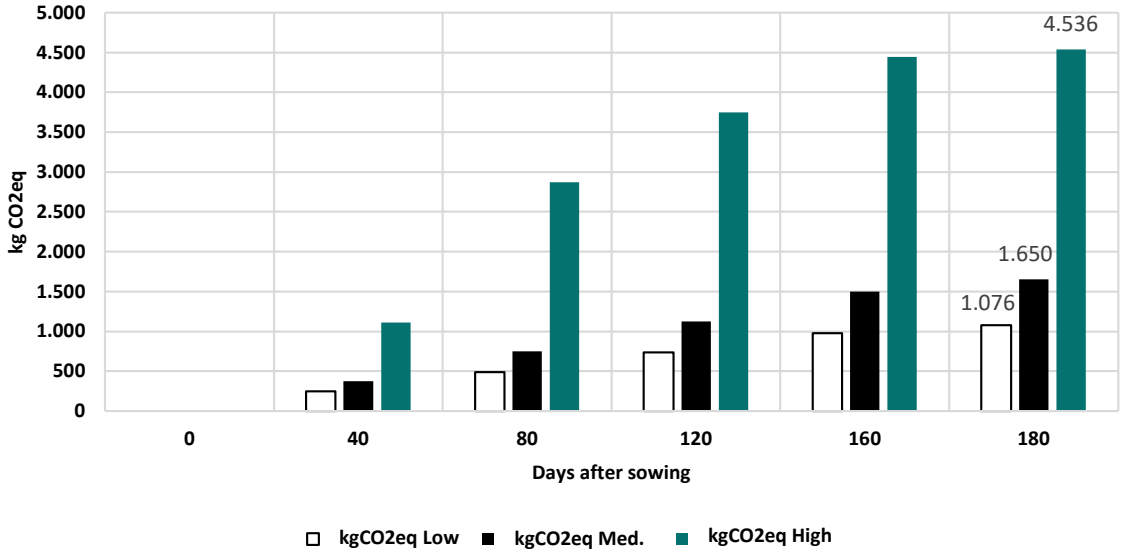

Source: Own elaboration based on the adjusted NL-CROP model.

6. Conclusions

NL-CROP is a non-linear model designed for assessing crop yield that has proven to be a powerful tool for agricultural research. Unlike traditional linear models that simplify the relationships between variables, NL-CROP captures the complexity of interactions between water, heat and climate stressors. This non-linear capacity provides a more precise representation of how these factors affect crop yield, which is essential for adaptation and sustainable management strategies. The main findings of the model's application in quinoa crops in Bolivia are the following:

Quinoa varieties adapted to local conditions, such as Pasankalla in Pampa Aullagas-Challapata, Quinua Real in Patacamaya, and Utasaya in Salinas de Garci Mendoza achieve greater foliage canopy development and produce higher yields compared to the conventional varieties. This is fundamental, given that these varieties have evolved in their particular surroundings and have developed characteristics allowing them to better tolerate the adverse climate conditions (such as drought and frost). Genetic adaptation not only improves plant capacity for capturing solar light and photosynthesizing, but also optimizes nutrient and water use, resulting in more efficient production.

However, quinoa yields does not solely depend on variety selection. The levels of soil compaction and fertility are key factors that influence crop growth and development. It has been observed that soils with adequate porosity provide greater yield, as they facilitate root development and the circulation of air and water. In contrast, compact soils limit root growth, restrict access to nutrients and water, and may cause stress in plants, resulting in a considerable reduction in productive potential. Thus, soil quality is an essential determining factor for maximizing quinoa production.

The relationship between the organic matter of the soil and yield is also critical. Soils with low organic matter content have yields of about 600 kg/ha, a level far below the maximum potential yield, even under normal climate conditions. Organic matter is essential for soil health, as it improves its structure, retains humidity and provides essential nutrients.

Without adequate management of soil fertility, quinoa production capacity is compromised; this emphasizes the need for implementing best agricultural practices that increase organic matter content.

Improvements in the soil's organic matter content allows reaching yields of over 800 kg/ha under normal climate conditions. This is because higher organic matter content improves the soil's capacity to retain water and nutrients, thus favoring more robust plant growth. Also, organic matter promotes biological activity in the soil, contributing to a more healthy and productive ecosystem. More robust soil also makes crops more resilient and resistant to the adverse effects of climate change, a factor that is crucial in a context where environmental conditions are increasingly uncertain.

In soils with adequate organic matter content, yield can surpass 1,400 kg/ha under dry land conditions, demonstrating the importance of proper soil management. This management implies not only adding organic matter, but also the implementation of practices such as crop rotation and the use of vegetation cover. On their part, water productivity improvements allow reaching yields of over 2,000 kg/ha, underscoring the interrelationship between soil management and water use efficiency, which is fundamental for agricultural production sustainability in the context of climate change.

The analyses of the climate change scenarios (Normal, La Niña and El Niño) reveal a significant impact in quinoa fresh biomass production. Across the period studied, a reduction of up to 13% is expected in production, considering a timeframe up to 2050. In particular, the La Niña scenario presents an increase of up to 32% attributable to the increase in precipitation, which together with efficiency in water use in quinoa production makes it likely that more grains be produced. On the other hand, the El Niño scenario shows a drastic fall of 37% as a result of prolonged drought and conditions of aridity that limit quinoa growth. These findings highlight this crop's vulnerability – despite its resistance to certain climate conditions – and emphasize the need for implementing adaptation strategies for mitigating the adverse effects of climate change.

Lastly, the CO2eq emissions analyses for the three simulated yield scenarios reveal a direct relationship between yield levels and greenhouse gas emissions (with the exception of the Pampa Aullagas case, which shows a U-shaped relationship, with the medium yield level generating the least amount of emissions). For example, for a phenological cycle of low yield in the Uyuni zone (269 KQH), emissions are 1,076 kg of CO2eq per hectare. For a medium yield trajectory (500 KQH), emissions of 1,650 kg of CO2eq are observed per hectare. Finally, for a high yield trajectory (756 KQH), emissions are at 4,536 kg of CO2eq per hectare. These emissions profiles reflect how yield levels affect greenhouse gas emissions. Low yield is associated with lower emissions because of a less intensive use of agricultural inputs, while increases in yield, particularly at high levels, carry with them substantial increases in emissions, attributable to the intensification of agricultural practices. This finding underscores the need to balance agricultural production with sustainable practices that minimize carbon emissions, fostering a more responsible approach to agricultural management.

The main conclusion of this work is that for achieving high quinoa yields and production sustainability it is fundamental to ensure adequate management of soil, water and agricultural practices. These three elements are interdependent and must be considered under the perspective of synergy for facing the challenges of climate change and optimizing production. Well managed soil is essential for robust quinoa development, as it directly influences the availability of nutrients and water retention capacity. However, soil quality alone does not guarantee good yield; it is equally crucial to implement efficient water management. Water availability, particularly in the context of climate change, can determine plant capacity to adequately grow and develop. Besides, proper agricultural practices, such as crop rotation and the use of vegetation cover complement these efforts to improve soil health and optimize the use of resources. These practices not only contribute towards increasing organic matter in the soil, but also foster a more balanced and resilient ecosystem.

The integration of these three elements – soil, water and agricultural practices – allow reaching yield trajectories that are not only high, but also sustainable. By doing this it is possible to implement production strategies that reduce greenhouse gas emissions and at the same time increase the capturing of carbon in the soil. This would be essential for mitigating the impacts of climate change, ensuring that quinoa production is not only viable presently, but also in the future. In summary, a holistic approach that takes into account the interrelationship between soil management, use of water, and agricultural practices would be essential for achieving sustainable and resilient production in the face of current environmental challenges.

Glossary

Base temperature (Tb): minimum temperature below which a crop does not grow (McMaster and Wilhelm, 1997)
Climate change scenarios (B1, A1T, B2, A1B, A2, A1F): different projections of future climate conditions, considering factors such as greenhouse gas emissions (IPCC, 2014)
CO2 concentration (CO2): amount of carbon dioxide present in the atmosphere (Myhre, *et al.*, 2013)
Coefficient of light extinction (k): parameter that describes the rate at which light attenuates as it passes through the vegetation canopy (Monsi and Saeki, 1953)
Coefficient of senescence at 360 ppm of CO2 (ks0): rate of senescence of the vegetation canopy at a concentration of 360 ppm of CO2 (Medlyn *et al.*, 1999)
Coefficient of vegetation canopy senescence (ks): parameter that describes the rate of senescence or ageing of the vegetation canopy (Goudriaan and Van Laar, 1994)
Degree days (°D): daily heat accumulation needed for crop development (McMaster and Wilhelm, 1997)
Extraterrestrial solar radiation (Ra): amount of solar energy that reaches the upper part of the atmosphere (Hargreaves and Samani, 1982)
Hargreaves-Samani method: method or model used to estimate maximum and minimum temperatures based on median temperature and solar radiation data (Hargreaves and Samani, 1982)
Harvest index (HI): ratio between economic yield and total biomass produced by a crop (Hay, 1995). Ratio between grain production and total biomass production (Sadras and Cassman, 2008)
Leaf area index (LAI): ratio between the total area of plant leaves and the area of the ground the plant occupies (Monsi and Saeki, 1953)
Maximum cover of vegetation canopy (CC_max): maximum cover that the vegetation canopy can reach (Goudriaan and Van Laar, 1994)
Mean daily temperature (Tmean): average of maximum and minimum daily temperatures (Hargreaves and Samani, 1982)
Minimum daily temperature (Tmin): lowest temperature recorded during the day (Hargreaves and Samani, 1982)
Optimal temperature (To): temperature at which the crop reaches it maximum rate of development (McMaster and Wilhelm, 1997)
Stomatal conductance (gs): capacity of plant stomas to exchange gases with the atmosphere (Medlyn *et al.*, 1999)
Stomatal conductance at 360 ppm of CO2 (gs0): stomatal conductance of a plant at a level of concentration of 360 ppm of CO2 (Medlyn *et al.*, 1999)
Vegetation canopy: upper layer of vegetation that covers the ground, made up of plant leaves and stems (Monsi and Saeki, 1953)
Vegetation canopy cover (CC): fraction of soil covered by the vegetation canopy (Goudriaan and Van Laar, 1994)
Vegetation canopy senescence (ks): rate of ageing or loss of vigor of the vegetation canopy (Goudriaan and Van Laar, 1994)
Water productivity (WP): amount of biomass produced per unit of water employed by a plant (Steduto *et al.*, 2012)

Bibliography

Allen, R. G., Pereira, L. S., Raes, D. & Smith, M. (1998). Crop Evapotranspiration-Guidelines for Computing Crop Water Requirements. *FAO Irrigation and drainage paper 56*. FAO, Roma, 300(9), D05109.

Antle, J. M., Stoorvogel, J. J. & Valdivia, R. O. (2014). New Parsimonious Simulation Methods and Tools to Assess Future Food and Environmental Security. *Philosophical Transactions of the Royal Society B: Biological Sciences*, 369(1639), p.201-208.

Asseng, S., Ewert, F., Rosenzweig, C., Jones, J. W., Hatfield, J. L., Ruane, A. C., Boote, K. J., Thorburn, P. J., Rötter, R. P., Cammarano, D. & Brisson, N. (2013). Uncertainty in Simulating Wheat Yields Under Climate Change. *Nature Climate Change*, 3(9), 827-832.

Boote, K. J., Jones, J. W., Mishoe, J. W. & Berger, R. D. (1983). Coupling Pests to Crop Growth Simulators to Predict Yield Reductions. *Phytopathology*, 73(11), 1581-1587.

Boote, K. J., Jones, J. W. y Pickering, N. B. (1996). Potential Uses and Limitations of Crop Models. *Agronomy Journal*, 88(5), 704-716.

Boulanger, J. P., Buckeridge, M. S., Castellanos, E., Poveda, G., Scarano, F. R. & Vicuña, S. (2014). *Impacts, Adaptation and Vulnerability, Contribution of Working Group II to the Fifth Assessment Report of the intergovernmental Panel on Climate Change.* Central and South America in Climate Change 2014. Cambridge, Reino Unido: Cambridge University y Nueva York, Estados Unidos de América. pp. 102-104.

Brouwer, C., Goffeau, A. & Heibloem, M. (1987). *Necesidades de agua de los cultivos*. Manual de campo n°3. Roma, Italia: FAO. pp. 79.

Challinor, A. J., Watson, J., Lobell, D. B., Howden, S. M., Smith, D. R. & Chhetri, N. (2014). A Meta-Analysis of Crop Yield Under Climate Change and Adaptation. *Nature Climate Change*, 4(4), 287-291.

Challinor, A. J., Wheeler, T. R., Craufurd, P. Q., Ferro, C. A. & Stephenson, D. B. (2007). Adaptation of Crops to Climate Change Through Genotypic Responses to Mean and Extreme Temperatures. *Agriculture, Ecosystems & Environment*, 119(1-2), 190-204.

Doorenbos, J. & Pruitt, W.O. (1976). Las necesidades de agua de los cultivos. *Estudio FAO: riego y drenaje*, 24, 194 p33.

Ewert, F., van Ittersum, M. K., Heckelei, T., Therond, O., Bezlepkina, I. & Andersen, E. (2011). Scale Changes and Model Linking Methods for Integrated Assessment of Agri-Environmental Systems. *Agriculture, Ecosystems & Environment*, 142(1-2), 6-17.

Fodor, N., Challinor, A., Droutsas, I., Ramirez-Villegas, J., Zabel, F., Koehler, A. K., & Foyer, C. H. (2017). Integrating Plant Science and Crop Modeling: Assessment of the Impact of Climate Change on Soybean and Maize Production. *Plant and Cell Physiology*, 58(11), 1833-1847. https://doi.org/10.1093/pcp/pcx141

Goudriaan, J., & Van Laar, H. H. (1994). *Modelling Potential Crop Growth Processes: Textbook with Exercises*. Springer Science & Business Media.

Hargreaves, G. H. & Samani, Z. A. (1982). Estimating Potential Evapotranspiration. *Journal of the Irrigation and Drainage Division*, 108(3), 225-230.

Hay, R. K. (1995). Harvest Index: A Review of Its Use in Plant Breeding and Crop Physiology. *Annals of Applied Biology*, 126(1), 197-216.

Hsiao, T. C. (1973). Plant Responses to Water Stress. *Annual Review of Plant Physiology*, 24(1), 519-570.

Holzworth, D. P., Snow, V., Janssen, S., Athanasiadis, I. N., Donatelli, M., Hoogenboom, G., White, J. W. & Thorburn, P. (2015). Agricultural Production Systems Modelling and Software: Current Status and Future Prospects. *Environmental Modelling & Software*, 72, 276-286.

Holzworth, D. P., Huth, N. I., deVoil, P. G., Zurcher, E. J., Herrmann, N. I., McLean, G., Chenu, K., van Oosterom, E. J., Snow, V., Murphy, C. & Moore, A. D. (2014). APSIM–Evolution Towards a New Generation of Agricultural Systems Simulation. *Environmental Modelling & Software*, 62, 327-350.

Hoogenboom, G., Jones, J. W., Wilkens, P. W., Porter, C. H., Boote, K. J., Hunt, L. A., Ligon, J. I., Ever, U.P.K.N., Gijsman, A. J. & Ritchie, J. T. (2010). *Decision Support System for Agrotechnology Transfer (DSSAT), Version 4.5 [CD-ROM].* University of Hawaii, Honolulu, Hawaii.

Intergovernmental Panel on Climate Change - IPCC. (2014). *Climate Change 2014: Synthesis Report. Contribution of Working Groups I, II and III to the fifth assessment report of the Intergovernmental Panel on Climate Change*. IPCC.

Jacobsen, M. Z., Delucchi, M. A., Barth, M., Bauer, S., Natalie, F., Gartz, S., & Mwabonje, O. (2011). Impacts of Climate Change on Regional Climate, Air Quality, and Human Health. *Wiley Interdisciplinary Reviews: Climate Change*, 2(5), 691-706.

Jacobsen, S. E. (2011). The Situation for Quinoa and its Production in Southern Bolivia: From Economic Success to Environmental Disaster. *Journal of Agronomy and Crop Science*, 197(5), 390-399.

Jones, J. W., Hoogenboom, G., Porter, C. H., Boote, K. J., Batchelor, W. D., Hunt, L. A., Wilkens, P. W., Singh, U., Gijsman, A. J. & Ritchie, J. T. (2003). The DSSAT Cropping System Model. *European Journal of Agronomy*, 18(3-4), 235-265.

Lobell, D. B. & Gourdji, S. M. (2012). The Influence of Climate Change on Global Crop Productivity. *Plant Physiology*, 160(4), 1686-1697.

Lobell, D. B. & Asseng, S. (2017). Comparing Estimates of Climate Change Impacts from Process-Based and Statistical Crop Models. *Environmental Research Letters*, 12(1), p.15.

McDowell, J. Z., & Hess, J. J. (2012). Accessing Adaptation: Multiple Stressors on Livelihoods in the Bolivian Highlands Under a Changing Climate. *Global Environmental Change*, 22(2), 342-352.

McMaster, G. S., & Wilhelm, W. W. (1997). Growing Degree-Days: One Equation, Two Interpretations. *Agricultural and Forest Meteorology*, 87(4), 291-300.

Medlyn, B. E., Dreyer, E., Ellsworth, D., Forstreuter, M., Harley, P. C., Kirschbaum, M. U., & Wang, S. (1999). Temperature Response of Parameters of a Biochemically-Based Model Photosynthesis. II. A Review of Experimental Data. *Plant, Cell & Environment*, 22(12), 1516-1526.

Monsi, M. & Saeki, T. (1953). Über den Lichtfaktor in den Pflanzengesellschaften und seine Bedeutung für die Stoffproduktion. *Japanese Journal of Botany*, 14(1), 22-52.

Monteith, J. L. (1985). *Evaporation from Land Surfaces: Progress in Analysis and Prediction Since 1948*. Advances in Evapotranspiration, Proc. National Conference on Advances in Evapotranspiration. Chicago, Illinois, Estados Unidos de América: Am. Soc Agric. Eng., St. Joseph, MI.

Morton, J. F. (2007). The Impact of Climate Change on Smallholder and Subsistence Agriculture. *Proceedings of the national Academy of Sciences*, *104*(50), 19680-5.

Myhre, G., Shindell, D., Bréon, F. M., Collins, W., Fuglestvedt, J., Huang, J. & Zhang, H. (2013). Anthropogenic and Natural Radiative Forcing. *Climate Change*, 423, 658-740.

Porter, J. R., Xie, L., Challinor, A. J., Cochrane, K., Howden, S. M., Iqbal, M. M., Lobell, D. B. and Travasso, M. I. (2014). Food Security and Food Production Systems. *Climate Change 2014: Impacts, Adaptation, and Vulnerability. Part A: Global and Sectoral Aspects*. Contribution of Working Group II to the Fifth Assessment Report of the Intergovernmental Panel on Climate Change (485-533). Cambridge University Press.

Raes, D., Steduto, P., Hsiao, T. C. & Fereres, E. (2009). Aquacrop – The FAO Crop Model to Simulate Yield Response to Water II. Main Algorithms and Software Description. *Agronomy Journal* 101, 438-447.

Rivington, M. & Koo, J. (2010). Linking Climate Change Modellers and Impact Assessment Users: A Review of Tools and Methods. *Integrated Assessment of Agriculture and Sustainable Development: Setting the Agenda for Science and Policy*. Wageningen, Países Bajos: Wageningen Academic Publishers, 45-56.

Rodríguez, C. (1980). *La radiación solar en la estimación de la evapotranspiración potencial*. Chapingo, México: Departamento de irrigación, Universidad Autónoma de Chapingo.

Rosenzweig, C., Jones, J. W., Hatfield, J. L., Ruane, A. C., Boote, K. J., Thorburn, P., Antle, J. M., Nelson, G. C., Porter, C., Janssen, S. & Asseng, S. (2013). The Agricultural Model Intercomparison and Improvement Project (AgMIP): Protocols and Pilot Studies. *Agricultural and Forest Meteorology*, 170,166-182.

Rötter, R. P., Carter, T. R., Olesen, J. E. & Porter, J. R. (2011). Crop–Climate Models Need an Overhaul. *Nature Climate Change*, 1(4), 175-177.

Rötter, R. P., Appiah, M., Fichtler, E., Kersebaum, K. C., Trnka, M. & Hoffmann, M. P. (2018). Linking Modelling and Experimentation to Better Capture Crop Impacts of Agroclimatic Extremes—A review. *Field Crops Research*, 221, 142-156.

Sadras, V. O., & Cassman, K. G. (2008). Yield Gaps in Grain Crops: Causes and Remedies. *Crop Physiology*, 495-517. Academic Press.

Semenov, M. A., & Stratonovitch, P. (2015). Adapting Wheat Ideotypes for Climate Change: Accounting for Uncertainties in CMIP5 Climate Projections. *Climate Research*, 65, 123-139. https://doi.org/10.3354/cr01297

Seguin B., Baelz, S., Monget, J. M. & Petit, V., (1982). Utilisation de la thermographie IR pour l'estimation de l'évaporation régionale. Mise au point méthologique sur le site de la Crau. *Agronomie*, 2, 7-16.

Shibu, M. E., Leffelaar, P. A., van Keulen, H. & Aggarwal, P. K. (2010). Quantitative Description of Soil Organic Matter Dynamics—A Review of Approaches with Reference to Rice-Based Cropping Systems. *Geoderma*, 155(1-2), 1-15. https://doi.org/10.1016/j.geoderma.2009.11.003

Steduto, P., Hsiao, T. C., Fereres, E., & Raes, D. (2012). Crop Yield Response to Water. *FAO Irrigation and drainage paper*, 66.

Stöckle, C. O., Donatelli, M. & Nelson, R. (2003). CropSyst, A Cropping Systems Simulation Model. *European Journal of Agronomy*, 18(3-4), 289-307.

Tao, F., Rötter, R. P., Palosuo, T., Díaz-Ambrona, C. G. H., Mínguez, M. I., Semenov, M. A., & Schulman, A. H. (2018). Contribution of Crop Model Structure: Parameters and Climate Projections to Uncertainty in Climate Change Impact Assessments. *Global Change Biology*, 24(3), 1291-1307. https://doi.org/10.1111/gcb.13965

Thornley, J. H., & France, J. (2007). *Mathematical Models in Agriculture: Quantitative Methods for the Plant, Animal and Ecological Sciences*. Cabi.

Trnka, M., Rötter, R. P., Ruiz-Ramos, M., Kersebaum, K. C., Olesen, J. E., Žalud, Z. & Semenov, M. A. (2014). Adverse Weather Conditions for European Wheat Production will Become More Frequent with Climate Change. *Nature Climate Change*, 4(7), 637-643.

Twomlow, S., Mugabe, F. T., Mwale, M., Delve, R., Nanja, D., Carberry, P. & Howden, M. (2008). Building Adaptive Capacity to Cope with Increasing Vulnerability due to Climatic Change in Africa–A New Approach. *Physics and Chemistry of the Earth,* A/B/C, 33(8-13), 780-787.

Valdivia, C., Thibeault, J., Gilles, J. L., García, M. & Seth, A. (2013). Climate Trends and Projections for the Andean Altiplano and Strategies for Adaptation. *Advances in Geosciences*, 33, 69-77.

White, J. W., Hoogenboom, G., Kimball, B. A. and Wall, G. W. (2011). Methodologies for Simulating Impacts of Climate Change on Crop Production. *Field Crops Research*, 124(3), 357-368.

ANNEX

A. Climograph: Pampa Aullagas and Challapata

The climate of Pampa Aullagas is classified as warm and temperate. Summers have an acceptable level of precipitation, while winters have very little. The climate is classified as Cwb according to the Köppen-Geiger climate classification. Temperature is on average 9.0 °C. Approximate yearly precipitation is 669 mm. Highest temperatures (on average) are in November, oscillating near 11.6 °C. July is the coldest month, with temperatures averaging 5.8 °C.

The month with the highest relative humidity is February (72.08%). The month with lowest relative humidity is June (26.02%). January is the month with the most number or rainy days (25.07). The month with less rain days is June (1.40). The least amount rain occurs in June, with an average of 6 mm. January has the most precipitation, with an average of 154 mm. Variation in precipitation between the driest and most humid months is 148 mm. Over the year, temperatures vary by 5.8 °C.

In Oruro, the month with the most daily hours of sun is November, with a median of 10.02 hours. In total, there are 310.49 hours of sun during this month. The month with the least hours of sun is January, with an average of 8.46 daily hours and a total of 262.32 hours in the month. In the year, Oruro has approximately 3,219.62 hours of sun. On average, there are 105.71 hours of sun per month.

Table 1: Seasonal climograph of Pampa Aullagas

	January	February	March	April	May	June	July	August	Sep.	October	November	December
Average temperature (°C)	10	9.8	9.6	9.3	7.8	6.4	5.8	7	8.8	10.5	11.6	11
Min. temperature (°C)	5.7	5.7	5	3.3	0.8	-0.4	-1.2	-0.6	1.1	3.4	4.9	5.8
Max. temperature (°C)	15.2	14.9	15.2	16	15.4	14.3	13.9	15.3	16.8	18	18.7	17.1
Precipitation (mm)	154	123	90	32	9	6	9	14	23	40	56	113
Humidity (%)	69%	72%	68%	53%	29%	26%	28%	29%	32%	36%	38%	55%
Rainy days (days)	19	17	16	8	2	1	2	3	4	8	10	16
Sunshine hours (hours)	6.9	6.5	6.9	8.5	9.6	9.5	9.5	9.8	9.9	10	10.1	8.5
Temperature range	Minimum	Maximum	Average									
Dry year	132.88	222.12	223.00									
Normal year	201.40	336.66	338.00									
Wet year	307.46	513.96	516.00									

Source: Own elaboration for the period 1991 - 2022, with information from Climate-data.org.

B. Climograph: Patacamaya

The region of Patacamaya is classified as ET according to the Köppen-Geiger climate classification; that is, a tundra climate. In the warmer months, this climate has median temperatures of between 0 °C and 10 °C. Vegetation consists

solely of herbs in the months that temperatures are above 0 °C (T for tundra[14]). Patacamaya may be considered ETH: an alpine tundra climate; that is, a tundra climate (ET), but at high altitude, such as that of cities like El Alto (Bolivia), Puno (Peru), and in a context outside the Andes, in Pagri (China).

Temperature is on average 6.8 °C, with an average precipitation of 820 mm. November is the warmest month of the year, with an average temperature of 9.0 °C. The coldest month (with an average of 4.2 °C) is July. Variation in temperature throughout the year is in the order of 4.8 °C.

The lowest relative humidity of the year occurs in June (42.99%). The month with the most humidity is February (74.45 %). The least number of rainy days tends to occur in June (4.30 days), and the rainiest days are observed in January (25.80 days). The driest month is June, with 17 mm of rain. On the opposite extreme is January, with median rainfall of 159 mm, making it the month with the most precipitation in the year. There is a difference of 142 mm in precipitation between the driest and most humid months.

The month with the most number of daily hours of sun is November, with a median of 9.06 hours. In total there are 280.71 hours of sun during this month. In January, the average is 8.05 hours, making it the month with the least daily hours of sun. The total number of sun hours in this month is 249.64. Finally, in Patacamaya there are about 2,958.34 hours of sun per year, with 97.13 hours as the monthly average.

Table 2: Seasonal climpograph of Patacamaya

	January	February	March	April	May	June	July	August	Sep.	October	November	December
Average temperature (°C)	7.8	7.7	7.5	6.9	5.8	4.8	4.2	5	6.3	7.8	9	8.6
Min. temperature (°C)	3.9	3.7	3	1.4	-1.1	-2.1	-2.7	-2	-0.3	1.6	3	3.9
Max. temperature (°C)	12.9	12.9	13.1	13.4	13.4	12.6	12.1	13.1	14.1	15	16	14.5
Precipitation (mm)	159	128	101	53	23	17	19	32	47	61	65	115
Humidity (%)	73%	74%	73%	64%	47%	43%	45%	48%	52%	54%	52%	64%
Rainy days (days)	19	17	17	11	4	3	4	6	8	10	11	16
Sunshine hours (hours)	6.4	6	6.2	7.3	9	9	8.9	9	8.8	9.1	9.3	8.1
Temperature range	Minimum	Maximum	Average									
Dry year	115.00	193.77	193.00									
Normal year	187.69	316.25	315.00									
Wet year	299.72	505.00	503.00									

Source: Own elaboration for the period 1991 - 2022, with information from Climate-data.org.

C. Climograph: Salinas de Garci Mendoza

The region of Salinas de Garci Mendoza[15] has a temperate and warm climate, an altitude of 3,732 masl, summers that are relatively rainy and dry winters. The climate, according to the Köppen-Geiger climate classification, is Cwb, or

[14] Tundra temperature is the thermal measure present in this region, with a cold and arid ecosystem. Tundra occurs near the poles. In the tundra, temperatures tend to be notably low, summers are short and cool, and winters are extremely cold.
[15] Several quinoa producer organizations operate in this zone: APQUISA, APRIOCA, AMEPROQUIR, ACIF.

isothermal (Cwb + i), a climate of the high sectors of the central Andes, and high zones of Mexico, Central America and the Horn of Africa. It is worth adding that isothermal (or equatorial) climate has low annual thermal amplitude, given that the difference between the hottest and coldest months is less than 5 °C. There are isothermal climates at high altitude, such as in the equatorial city of Quito (Ecuador), Misti (Peru) and the Bolivia Altiplano.

In Salinas de Garci Mendoza, the lowest value of relative humidity occurs in June (13.47%), and the highest relative humidity takes place in February (64.11%). On average, the month with the least number of rainy days is June (0.27 days) and the month with the most number of rainy days is January (19.30 days). Median annual temperature is 8.47 °C, with a maximum of 15.38 °C and a minimum of 1.7 °C. Maximum annual precipitation is 505 mm. The driest month is May (1 mm of precipitation), and the month with the most precipitation is January, with an average 158 mm. With a median precipitation of 303 mm per year, Salinas de Garci Mendoza has a water deficit of between 280 and 332 mm per year.

Table 3: Seasonal climpograph of Salinas de Garci Mendoza

	January	February	March	April	May	June	July	August	Sep.	October	November	December
Average temperature (°C)	10	9.7	9.5	9	6.5	5	4.4	6.2	8.2	10.1	11.4	11.6
Min. temperature (°C)	5.2	4.9	3.9	2.2	-0.7	-2	-2.5	-1.5	0.1	2.2	3.5	5.1
Max. temperature (°C)	15.7	15.2	15.5	15.7	13.7	12.3	11.7	13.8	16	17.8	18.9	18.3
Precipitation (mm)	158	135	77	15	1	1	3	5	4	10	20	76
Humidity (%)	56%	64%	56%	33%	17%	13%	15%	14%	15%	16%	18%	32%
Rainy days (days)	14	13	10	3	0	0	1	1	1	2	3	8
Sunshine hours (hours)	8.5	7.8	8.3	9.7	9.9	9.8	9.8	10.2	10.6	11.1	11.4	10.6
Temperature range	Minimum	Maximum	Average									
Dry year	76.00	159.17	95.50									
Normal year	133.70	280.00	168.00									
Wet year	241.13	505.00	303.00									

. Source: Own elaboration for the period 1991 - 2022, with information from Climate-data.org.

D. Climograph: Uyuni, Colchacani and Pulacayo

This section presents the climograph for this zone of the study; it is a climate record with multiple entries that summarizes the values of precipitation, temperature, humidity, sun days and rain days. The information is based on historical records spanning 30-35 years (or more), obtained at the weather stations of the Bolivian Altiplano.

The climograph allows knowing the conditions based on which the phenological cycle of the crop is developed. Low temperatures particularly affect the germination phases, as a minimum of - 4 °C is needed, but they also affect the flowering phase, causing low production of pollen and consequently plant sterility. In the branching phase, the plants do not have problems of note with falls in temperature down to - 4 °C.

On the other hand, high temperatures affect the physiological process of the plant, making its grain production process accelerate, while it seeks to ensure its survival. We also assume flower abortion with median optimal temperatures from 5 to 15 °C and thermal oscillation of 5 to 7 °C. Finally, when there are extreme drops in temperature, below - 4°C, cellular physiological changes occur, as well as ruptures of plasma due to the presence of intercellular ice crystals.

The Uyuni region is in the southern hemisphere at 3,700 masl. The month with the highest relative humidity is February (60.74%), while the month with the least is June (14.59%). The month with the most number of rainy days is January (19.40), and the one with the least is June (0.33).

The climate is classified as Cwb according to the Köppen-Geiger climate classification; that is, temperate with dry winters. The months from December to March have much more rain than the others, with a median annual temperature of 7.8 °C. With a median temperature of 11.8 °C, December is the warmest month of the year. With an average of 2.7 °C, July is the coldest month, and annual temperature variation is of about 9.1 °C.

The difference in the level of precipitation between the driest and most humid months is 145 mm. The approximate level of median precipitation is 445 mm, with the lowest level occurring in June, with an average of 1 mm. In January, precipitation reaches its peak, with an average of 146 mm.

The month with the most hours of sun daily is November, with a median of 11.05 and a total of 342.59 sun hours. The month with the least number of daily sun hours is January, with an average of 10.45 per day. In total there are 323.8 sun hours during this month. Uyuni has approximately 3,611.57 hours of sun throughout the year, with a monthly average of 118.63 hours.

Table 4: Seasonal climpograph of Uyuni

	January	February	March	April	May	June	July	August	Sep.	October	November	December
Average temperature (°C)	10.8	10.3	10	8.4	4.7	3.1	2.7	4.4	6.7	9.2	11	11.8
Min. temperature (°C)	5.1	5	3.7	0.8	-2.6	-3.4	-3.8	-3.4	-2.1	-0.1	1.8	4.5
Max. temperature (°C)	16.9	16.2	16.6	15.9	12.7	11	10.6	12.8	15.2	17.4	18.8	18.8
Precipitation (mm)	146	112	60	13	2	1	2	4	4	11	19	71
Humidity (%)	54%	61%	52%	31%	18%	15%	16%	15%	15%	17%	18%	34%
Rainy days (days)	15	13	9	2	0	0	0	1	1	2	3	8
Sunshine hours (hours)	8.7	8.2	8.8	9.8	9.9	9.8	9.8	10.2	10.6	11.1	11.4	10.4
Temperature range	Mínimo	Máximo	Medio									
Dry year	88.00	315.00	100.00									
Normal year	156.00	400.00	160.00									
Wet year	246.00	493.00	280.00									

Source: Own elaboration for the period 1991 - 2022, with information from Climate-data.org.

CO2 concentration

For complementing the analysis, we incorporate into the model different CO2 concentration scenarios and their impact on biomass and grain production. CO2 concentration in the atmosphere:

a. Historical value (1959-2021):

$$CO_2 = 315.7 + 2.06 \cdot (y - 1959) \quad (19),$$

where:

CO_2 is the concentration of carbon dioxide in the atmosphere (ppm);
y is the year.

b. Climate change scenarios:

Scenario B1: $CO_2 = 600\ ppm$
Scenario A1T: $CO_2 = 700\ ppm$
Scenario B2: $CO_2 = 800\ ppm$
Scenario A1B: $CO_2 = 850\ ppm$
Scenario A2: $CO_2 = 1250\ ppm$
Scenario A1F: $CO_2 = 1550\ ppm$

The effect of CO2 concentration on the production of biomass and grain is a stomatal conductance case (g_s) shown in Equation (20):

$$g_s = g_{so}\left[1 + 0.3\frac{(CO_2 - 360)}{360}\right] \quad (20),$$

where g_{so} is stomatal conductance at 360 ppm of CO2.

In the case of vegetation canopy senescence, (k_s), we have Equation (21):

$$k_s = k_{so}\left[1 - 0.2\frac{(CO_2 - 360)}{360}\right] \quad (21),$$

where k_{so} is the senescence coefficient at 360 ppm of CO2.

In terms of water productivity (*WP*), we have (Equation 22):

$$WP = WP_0\left[1 - 0.4\frac{(CO_2 - 360)}{360}\right] \quad (22),$$

where WP_0 is water productivity at 360 ppm of CO2.

And, with a harvest index (H) as shown in Equation (23):

$$H = H_0\left[1 - 0.1\frac{(CO_2 - 360)}{360}\right] \quad (23),$$

where H_0 is the harvest index at 360 ppm of CO2.

By incorporating these equations, the model will be able to simulate quinoa crop growth and development under different scenarios of CO2 concentration, considering the effects of stomatal conductance, vegetation canopy senescence, water productivity and the harvest index.